

# Adiabatic elimination for composite open quantum systems: reduced model formulation and numerical simulations

Francois-Marie Le Régent\*

*Alice&Bob, 53 boulevard du Général Martial Valin, 75015 Paris and  
Laboratoire de Physique de l'Ecole normale supérieure, ENS-PSL,  
CNRS, Inria, Mines-Paris - PSL, Université PSL, Paris, France.*

Pierre Rouchon†

*Laboratoire de Physique de l'Ecole normale supérieure, ENS-PSL,  
CNRS, Inria, Mines-Paris - PSL, Université PSL, Paris, France.*

A numerical method is proposed for simulation of composite open quantum systems. It is based on Lindblad master equations and adiabatic elimination. Each subsystem is assumed to converge exponentially towards a stationary subspace, slightly impacted by some decoherence channels and weakly coupled to the other subsystems. This numerical method is based on a perturbation analysis with an asymptotic expansion. It exploits the formulation of the slow dynamics with reduced dimension. It relies on the invariant operators of the local and nominal dissipative dynamics attached to each subsystem. Second-order expansion can be computed only with local numerical calculations. It avoids computations on the tensor-product Hilbert space attached to the full system. This numerical method is particularly well suited for autonomous quantum error correction schemes. Simulations of such reduced models agree with complete full model simulations for typical gates acting on one and two cat-qubits (Z, ZZ and CNOT) when the mean photon number of each cat-qubit is less than 8. For larger mean photon numbers and gates with three cat-qubits (ZZZ and CCNOT), full model simulations are almost impossible whereas reduced model simulations remain accessible. In particular, they capture both the dominant phase-flip error-rate and the very small bit-flip error-rate with its exponential suppression versus the mean photon number.

## CONTENTS

I. Introduction	1	A. High-order expansion and simulations	16
II. Second-order expansion and Z-gate simulations	2	1. Expansion order exceeding 2	16
A. Invariant manifold and slow dynamics approximation	2	2. Z-gate simulations up to order 5	16
B. Z-gate simulations for a single cat-qubit	4	B. Second-order approximation with slow time dependency	16
III. Composite systems and ZZ/ZZZ-gate simulations	6	C. Time discretization of continuous-time quantum master equation	17
A. Second-order approximation with only local computations	6	D. Adiabatic elimination in discrete-time	18
B. ZZ gate	8	1. Single system	18
C. ZZZ gate	10	2. Composite systems	19
IV. Composite systems with an unstabilized component	10	E. Propagator simulation results	20
A. Second-order approximation	10	F. Leakage computation	20
B. CNOT gate	12	1. Single-mode leakage	20
C. CCNOT gate	12	2. Composite-system leakage	20
V. Concluding remarks	13	3. Hybrid system leakage	21
VI. Acknowledgments	13	G. Analytic error models	21
References	14	1. Z and ZZ gates	22
		2. ZZZ gate	22

## I. INTRODUCTION

Quantum processors rely on controllable quantum systems [1, 2], which are prone to errors, mainly due to the environment, and therefore require quantum error correction with a very large number of physical resources to

\* francois-marie.le-regent@alice-bob.com

† pierre.rouchon@minesparis.psl.eu

operate [3–9]. To reduce errors hence resource overheads, bosonic encodings have emerged, taking advantage of the infinitely large Hilbert space of harmonic oscillators for intrinsic autonomous error correction [10–15].

However, with such infinite systems, capturing the physics of gates and error processes becomes challenging. Classical numerical simulations require taking into account many states of the Hilbert space to model their dynamics [16, 17]. In addition, simulations of composite systems with more than two modes are often intractable, as the dimension of the total Hilbert space is exponential in the number of modes, each mode description requiring an Hilbert-space of large dimension [18, 19]. Model reduction techniques have thus been developed and can use a more suitable basis of the Hilbert space to describe the physical systems via a subsystem decomposition [19–21].

Other methods, such as adiabatic elimination, are used to analyze the dynamics of open and dissipative quantum systems under a deterministic Lindblad master equation. Adiabatic elimination corresponds to a perturbation technique known in dynamical and control system theory as singular perturbations for slow/fast systems. It is related to the Tikhonov approximation theorem (see, e.g., [22, 23]) and its coordinate-free formulation due to Fenichel [24] with the notion of invariant slow manifold of a dynamical system having two time-scales dynamics: the fast and exponentially converging ones and the slow ones of reduced dimension. Adiabatic elimination produces low dimensional dynamical models via the derivation of the slow differential equation governing the evolution on the invariant slow manifold [25–30].

In this context, we propose here an original numerical method based on adiabatic elimination to simulate on a classical computer, quantum master equations modeling composite systems having fast and local dissipation with weak coupling between the sub-systems and slow decoherence. These calculations are simplified by exploiting the invariant operators attached the fast dynamics. The resulting reduced model of the slow evolution yields an efficient numerical method for classical simulations of composite slow/fast systems having a too large Hilbert space for brute-force numerical integration of the original slow/fast master equations.

Such low-dimensional reduced models are particularly well suited for numerical simulation of autonomous quantum error correction schemes developed for bosonic codes. For cat-qubit systems, several numerical simulations based on formal adiabatic calculations and their numerical implementations are presented. They succeed in capturing both the macroscopic phase-flip errors associated with finite gate time and photon losses (the dominant error process for harmonic oscillators), and also the exponentially small bit-flip errors known to be much harder to estimate [18, 19].

In Section II, we recall for quantum master differential equations the formalism of stationary states and invariant operators, and detail the formal adiabatic calculations up to the second-order of the continuous-time slow

dynamics. These formal calculations are then exploited numerically to simulate the resulting second-order slow model for a Z-gate on a single cat-qubit. Comparison with numerical simulations of the full slow/fast model are given. In Section III, we then extend these second-order calculations to a composite system of locally stabilized subsystems. We show how their numerical implementations can be done with only local computations on the Hilbert space of each subsystem. This avoids computations on the full Hilbert space of the complete system. For the composite system made of two (resp. three) cat-qubits, numerical simulations of a ZZ (resp. ZZZ) gate are presented with an emphasis on the different error rates. In Section IV, we adapt this simulation method to composite systems for which one of the subsystem is not stabilized. For two (resp. three) cat-qubits, numerical simulations provide the error probabilities of a CNOT (resp. CCNOT) gate where the target qubit is not stabilized during the gate. Sections in appendix are mainly devoted to high-order adiabatic calculations, additional simulation results, discrete-time formulations with Kraus maps and the derived time-discretization schemes underlying the numerical simulations.

## II. SECOND-ORDER EXPANSION AND Z-GATE SIMULATIONS

### A. Invariant manifold and slow dynamics approximation

The calculations of this sub-section are very similar to section 2 and 3 of [31].

Consider the time-varying density operator  $\rho_t$  on underlying Hilbert space  $\mathcal{H}$  obeying to the following dynamics

$$\frac{d}{dt}\rho_t = \mathcal{L}_0(\rho_t) + \epsilon\mathcal{L}_1(\rho_t) \quad (1)$$

with two Gorini–Kossakowski–Sudarshan–Lindblad (GKSL) linear superoperators  $\mathcal{L}_0$  and  $\mathcal{L}_1$  where  $\epsilon$  is a small positive parameter. For  $\sigma = 0, 1$  one has

$$\begin{aligned} \mathcal{L}_\sigma(\rho) = & -i[\hat{H}_\sigma, \rho] + \sum_\nu \hat{L}_{\sigma,\nu}\rho\hat{L}_{\sigma,\nu}^\dagger - \frac{1}{2}\left(\hat{L}_{\sigma,\nu}^\dagger\hat{L}_{\sigma,\nu}\rho + \rho\hat{L}_{\sigma,\nu}^\dagger\hat{L}_{\sigma,\nu}\right) \end{aligned} \quad (2)$$

with  $\hat{H}_\sigma$  Hermitian operator and  $\hat{L}_{\sigma,\nu}$  any operator not necessarily Hermitian.

Assume that for  $\epsilon = 0$  and any initial condition  $\rho_0$ , the solution of (1) converges exponentially towards a steady-state depending a priori on  $\rho_0$ . This means that we have a quantum channel  $\bar{\mathcal{K}}_0$  defined by

$$\lim_{t \rightarrow +\infty} e^{t\mathcal{L}_0}(\rho_0) \triangleq \bar{\mathcal{K}}_0(\rho_0). \quad (3)$$

The range of  $\bar{\mathcal{K}}_0$  is denoted by  $\mathcal{D}_0$ , the set of steady-states corresponding to the kernel of  $\mathcal{L}_0$ , a vector subspace of Hermitian operators. Denote by  $\bar{d}$  the dimension of  $\mathcal{D}_0$  and consider an orthonormal basis of  $\mathcal{D}_0$  made of  $\bar{d}$  Hermitian operators  $\hat{S}_1, \dots, \hat{S}_{\bar{d}}$  such that  $\text{Tr}(\hat{S}_d \hat{S}_{d'}) = \delta_{d,d'}$ .

To each  $\hat{S}_d$  is associated an invariant operator

$$\hat{J}_d = \lim_{t \rightarrow +\infty} e^{t\mathcal{L}_0^*}(\hat{S}_d)$$

being a steady-state of the adjoint dynamics (according to the Frobenius Hermitian product)  $\frac{d}{dt}\hat{J} = \mathcal{L}_0^*(\hat{J})$  where  $\mathcal{L}_0^*$  is the adjoint of  $\mathcal{L}_0$  (see, e.g., [32]). For any solution  $\rho_t$  of (1) with  $\epsilon = 0$ ,  $\text{Tr}(\hat{J}_d \rho_t)$  is constant. This gives the following expression for  $\bar{\mathcal{K}}_0$ :

$$\lim_{t \rightarrow +\infty} \rho_t = \sum_{d=1}^{\bar{d}} \text{Tr}(\hat{J}_d \rho_0) \hat{S}_d \triangleq \bar{\mathcal{K}}_0(\rho_0). \quad (4)$$

Moreover,  $\text{Tr}(\hat{J}_d \hat{S}_{d'}) = \delta_{d,d'}$  since for any  $t > 0$

$$\begin{aligned} \text{Tr}(e^{t\mathcal{L}_0^*}(\hat{S}_d) \hat{S}_{d'}) &= \text{Tr}(\hat{S}_d e^{t\mathcal{L}_0}(\hat{S}_{d'})) \\ &= \text{Tr}(\hat{S}_d \hat{S}_{d'}) = \delta_{d,d'} \end{aligned} \quad (5)$$

using the fact that  $e^{t\mathcal{L}_0}(\hat{S}_{d'}) = \hat{S}_{d'}$ .

For  $\epsilon > 0$  and small, Eq. (1) also admits a  $\bar{d}$  dimensional linear subspace denoted by  $\mathcal{D}_\epsilon$  invariant and close to  $\mathcal{D}_0$  (see [33] for a mathematical justification in finite dimension). Thus, the set of  $\bar{d}$  real variables

$$x_1 = \text{Tr}(\hat{J}_1 \rho), \dots, x_{\bar{d}} = \text{Tr}(\hat{J}_{\bar{d}} \rho)$$

can be chosen to be local coordinates on  $\mathcal{D}_\epsilon$ : any density operators  $\rho \in \mathcal{D}_\epsilon$  reads  $\rho = \sum_{d=1}^{\bar{d}} x_d \hat{S}_d(\epsilon)$  with the perturbed basis  $\hat{S}_1(\epsilon), \dots, \hat{S}_{\bar{d}}(\epsilon)$  and  $\bar{d}$  real numbers  $x_d$ .

Invariance of  $\mathcal{D}_\epsilon$  with respect to (1) means that, if at some time  $t$ , the solution  $\rho_t$  of the perturbed system (1) belongs to  $\mathcal{D}_\epsilon$ , it remains on  $\mathcal{D}_\epsilon$  at any time:  $\frac{d}{dt}\rho_t = (\mathcal{L}_0 + \epsilon\mathcal{L}_1)(\rho_t)$  with  $\rho_t = \sum_{d=1}^{\bar{d}} x_d(t) \hat{S}_d(\epsilon)$ . For any  $(x_1(t), \dots, x_{\bar{d}}(t)) \in \mathbb{R}^{\bar{d}}$ , this invariance property reads

$$\sum_{d=1}^{\bar{d}} \frac{dx_d}{dt} \hat{S}_d(\epsilon) = (\mathcal{L}_0 + \epsilon\mathcal{L}_1) \left( \sum_{d=1}^{\bar{d}} x_d \hat{S}_d(\epsilon) \right). \quad (6)$$

Thus, for any  $d \in \{1, \dots, \bar{d}\}$ ,  $\frac{dx_d}{dt}$  depends linearly on  $x = (x_1, \dots, x_{\bar{d}})$ , i.e.

$$\frac{d}{dt}x_d = \sum_{d'} F_{d,d'}(\epsilon) x_{d'}. \quad (7)$$

The invariance condition reads now,

$$\begin{aligned} \forall (x_1, \dots, x_{\bar{d}}) \in \mathbb{R}^{\bar{d}}, \quad \sum_{d,d'} x_{d'} F_{d,d'}(\epsilon) \hat{S}_d(\epsilon) \\ \equiv \sum_d x_d (\mathcal{L}_0 + \epsilon\mathcal{L}_1)(\hat{S}_d(\epsilon)) \end{aligned} \quad (8)$$

which is equivalent to

$$\forall d \in \{1, \dots, \bar{d}\}, \quad \sum_{d'=1}^{\bar{d}} F_{d',d}(\epsilon) \hat{S}_{d'}(\epsilon) = (\mathcal{L}_0 + \epsilon\mathcal{L}_1)(\hat{S}_d(\epsilon)). \quad (9)$$

With the asymptotic expansion

$$F_{d,d'}(\epsilon) = \sum_{n \geq 0} \epsilon^n F_{d,d'}^{(n)}, \quad \hat{S}_d(\epsilon) = \sum_{n \geq 0} \epsilon^n \hat{S}_d^{(n)} \quad (10)$$

one can compute recursively  $F_{d,d'}^{(n)}$  and  $\hat{S}_d^{(n)}$  from  $F_{d,d'}^{(m)}$  and  $\hat{S}_d^{(m)}$  with  $m < n$ . The recurrence relationship is based on the identification of terms with same orders versus  $\epsilon$  in the following equations

$$\begin{aligned} \forall d \in \{1, \dots, \bar{d}\}, \quad \sum_{d'=1}^{\bar{d}} \left( \sum_{n \geq 0} \epsilon^n F_{d',d}^{(n)} \right) \left( \sum_{n' \geq 0} \epsilon^{n'} \hat{S}_{d'}^{(n')} \right) \\ = (\mathcal{L}_0 + \epsilon\mathcal{L}_1) \left( \sum_{n \geq 0} \epsilon^n \hat{S}_d^{(n)} \right). \end{aligned} \quad (11)$$

The zero-order condition is satisfied with  $F_{d,d'}^{(0)} = 0$  and  $\hat{S}_d^{(0)} = \hat{S}_d$ . First-order condition reads

$$\forall d \in \{1, \dots, \bar{d}\}, \quad \sum_{d''=1}^{\bar{d}} F_{d'',d}^{(1)} \hat{S}_{d''}^{(0)} = \mathcal{L}_0(\hat{S}_d^{(1)}) + \mathcal{L}_1(\hat{S}_d^{(0)}). \quad (12)$$

Left multiplication by operator  $\hat{J}_{d'}$  and taking the trace yields

$$F_{d',d}^{(1)} = \text{Tr}(\hat{J}_{d'} \mathcal{L}_1(\hat{S}_d^{(0)})) \quad (13)$$

since  $\text{Tr}(\hat{J}_{d'} \hat{S}_{d''}^{(0)}) = \delta_{d',d''}$  and  $\text{Tr}(\hat{J}_{d'} \mathcal{L}_0(\hat{W})) = 0$  for any operator  $\hat{W}$  because  $\mathcal{L}_0^*(\hat{J}_{d'}) = 0$ . Thus,  $\hat{S}_d^{(1)}$  is a solution  $\hat{X}$  of the following equation:

$$\begin{aligned} \mathcal{L}_0(\hat{X}) &= \sum_{d'} \text{Tr}(\hat{J}_{d'} \mathcal{L}_1(\hat{S}_d^{(0)})) \hat{S}_{d'} - \mathcal{L}_1(\hat{S}_d^{(0)}) \\ &= \bar{\mathcal{K}}_0(\mathcal{L}_1(\hat{S}_d^{(0)})) - \mathcal{L}_1(\hat{S}_d^{(0)}) \end{aligned} \quad (14)$$

where the quantum channel  $\bar{\mathcal{K}}_0$  is defined in (3). Following [28], the general solution  $\hat{X}$  is given by the absolutely converging integral,

$$\hat{X} = \int_0^{+\infty} e^{s\mathcal{L}_0} \left( \mathcal{L}_1(\hat{S}_d^{(0)}) - \bar{\mathcal{K}}_0(\mathcal{L}_1(\hat{S}_d^{(0)})) \right) ds + \widehat{W} \quad (15)$$

where  $\widehat{W}$  belongs to  $\mathcal{D}_0$  the kernel of  $\mathcal{L}_0$ . We consider the solution with  $\widehat{W} = 0$  and thus

$$\hat{S}_d^{(1)} = \int_0^{+\infty} e^{s\mathcal{L}_0} \left( \mathcal{L}_1(\hat{S}_d^{(0)}) - \bar{\mathcal{K}}_0(\mathcal{L}_1(\hat{S}_d^{(0)})) \right) ds \quad (16)$$

where for all  $d'$ ,  $\text{Tr}(\hat{J}_{d'} \hat{S}_d^{(1)}) = 0$ . The superoperator  $\bar{\mathcal{R}}_0$  defined for any operator  $\hat{W}$  by

$$\bar{\mathcal{R}}_0(\hat{W}) = \int_0^{+\infty} e^{s\mathcal{L}_0} (\hat{W} - \bar{\mathcal{K}}_0(\hat{W})) ds \quad (17)$$

provides thus the unique solution  $\hat{X} = \bar{\mathcal{R}}_0(\hat{W})$  of  $\mathcal{L}_0(\hat{X}) = \bar{\mathcal{K}}_0(\hat{W}) - \hat{W}$  such that for all  $d$ ,  $\text{Tr}(\hat{J}_d \hat{X}) = 0$ . To summarize, the first-order terms in  $\epsilon$  are

$$F_{d',d}^{(1)} = \text{Tr}(\hat{J}_{d'} \mathcal{L}_1(\hat{S}_d^{(0)})) \quad \text{and} \quad \hat{S}_d^{(1)} = \bar{\mathcal{R}}_0(\mathcal{L}_1(\hat{S}_d)). \quad (18)$$

Second-order conditions are

$$\forall d \in \{1, \dots, \bar{d}\}, \quad \sum_{d''=1}^{\bar{d}} F_{d'',d}^{(1)} \hat{S}_{d''}^{(1)} + F_{d'',d}^{(2)} \hat{S}_{d''}^{(0)} = \mathcal{L}_0(\hat{S}_d^{(2)}) + \mathcal{L}_1(\hat{S}_d^{(1)}). \quad (19)$$

Left multiplication by operator  $\hat{J}_{d'}$  and taking the trace yields:

$$F_{d',d}^{(2)} = \text{Tr}(\hat{J}_{d'} \mathcal{L}_1(\hat{S}_d^{(1)})) = \text{Tr}(\mathcal{L}_1^*(\hat{J}_{d'}) \hat{S}_d^{(1)}). \quad (20)$$

Computations similar to the ones performed for the first-order conditions yield

$$\hat{S}_d^{(2)} = \bar{\mathcal{R}}_0 \left( \mathcal{L}_1(\hat{S}_d^{(1)}) - \sum_{d''=1}^{\bar{d}} F_{d'',d}^{(1)} \hat{S}_{d''}^{(1)} \right). \quad (21)$$

Higher order formulae are given in appendix A 1. The equivalent of Eqs. (18) and (20) for a slow time dependency are detailed in appendix B and for discrete-time setting in appendix D 1.

## B. Z-gate simulations for a single cat-qubit

For a cat-qubit system [18, 34, 35], the quantum state  $\rho$  is attached to a harmonic oscillator. It is confined through an engineered two-photon driven dissipation process to have its range close to a two-dimensional subspace spanned by two coherent wave functions  $|\pm\alpha\rangle$  of opposite complex amplitudes  $\pm\alpha$ . This means that the support of  $\rho$  remains close to the sub-Hilbert space of dimension 2 spanned by the orthonormal wave functions (the Schrödinger cat states)

$$|\mathcal{C}_\alpha^\pm\rangle := \mathcal{N}_\pm(|\alpha\rangle \pm |-\alpha\rangle), \quad (22)$$

where  $\mathcal{N}_\pm = (2(1 \pm \exp(-2|\alpha|^2)))^{-1/2}$  are normalizing constants. The computational wave-function are given by the following equations:

$$|0\rangle_C = (|\mathcal{C}_\alpha^+\rangle + |\mathcal{C}_\alpha^-\rangle)/\sqrt{2} = |\alpha\rangle + \mathcal{O}(e^{-2|\alpha|^2}) \quad (23)$$

$$|1\rangle_C = (|\mathcal{C}_\alpha^+\rangle - |\mathcal{C}_\alpha^-\rangle)/\sqrt{2} = |-\alpha\rangle + \mathcal{O}(e^{-2|\alpha|^2}). \quad (24)$$

The engineered two-photon driven dissipation process can be effectively modeled by as single Lindblad term of the form

$$\mathcal{L}_0(\rho) = \mathcal{D}_{\hat{L}_0}(\rho) \triangleq \left( \hat{L}_0 \rho \hat{L}_0^\dagger - \frac{1}{2}(\hat{L}_0^\dagger \hat{L}_0 \rho + \rho \hat{L}_0^\dagger \hat{L}_0) \right) \quad (25)$$

with  $\hat{L}_0 = \sqrt{\kappa_2}(\hat{a}^2 - \alpha^2)$ ,  $\kappa_2 > 0$  and  $\hat{a}$  being the photon annihilator operator. Such a process can be engineered in a superconducting platform [34]. It stabilizes exponentially the cat-qubit subspace corresponding then to  $\mathcal{D}_0$  (called the code subspace in the context of bosonic codes) [36]. Its real dimension is  $\bar{d} = 4$  with the following orthonormal operator basis

$$\begin{aligned} \hat{S}_1 &= (|\mathcal{C}_\alpha^+\rangle \langle \mathcal{C}_\alpha^+| + |\mathcal{C}_\alpha^-\rangle \langle \mathcal{C}_\alpha^-|)/\sqrt{2}, \\ \hat{S}_2 &= (|\mathcal{C}_\alpha^+\rangle \langle \mathcal{C}_\alpha^+| - |\mathcal{C}_\alpha^-\rangle \langle \mathcal{C}_\alpha^-|)/\sqrt{2}, \\ \hat{S}_3 &= (i|\mathcal{C}_\alpha^+\rangle \langle \mathcal{C}_\alpha^-| - i|\mathcal{C}_\alpha^-\rangle \langle \mathcal{C}_\alpha^+|)/\sqrt{2}, \\ \hat{S}_4 &= (|\mathcal{C}_\alpha^+\rangle \langle \mathcal{C}_\alpha^-| + |\mathcal{C}_\alpha^-\rangle \langle \mathcal{C}_\alpha^+|)/\sqrt{2}. \end{aligned} \quad (26)$$

Among the errors and decoherence processes, the dominant one is the undesired single-photon loss, modelled by

$$\mathcal{D}_{\sqrt{\kappa_1}\hat{a}}(\rho) \triangleq \kappa_1 (\hat{a}\rho\hat{a}^\dagger - \frac{1}{2}(\hat{a}^\dagger\hat{a}\rho + \rho\hat{a}^\dagger\hat{a})) \quad (27)$$

where  $\kappa_1 > 0$ . Usually the ratio  $\kappa_1/\kappa_2$  is small:  $\kappa_1$  is the single-photon loss rate, much smaller than  $\kappa_2$  the rate of mechanism stabilizing the code-space  $\mathcal{D}_0$ .

A Z-gate corresponds to a unitary transformation exchanging  $|\mathcal{C}_\alpha^+\rangle$  and  $|\mathcal{C}_\alpha^-\rangle$ . Following [34, 37], it can be approximately engineered via the propagator of time duration  $T > 0$  associated to the Hamiltonian  $\hat{H}_1 = \epsilon_Z (\hat{a} + \hat{a}^\dagger)$  where  $\epsilon_Z = \frac{\pi}{4\alpha T}$  has to be much smaller than  $\kappa_2$ . The superoperators  $\mathcal{L}_0$  and  $\mathcal{L}_1$  corresponding here to Eq. (1) are thus

$$\begin{aligned} \mathcal{L}_0(\rho) &= \kappa_2 D_{\hat{a}^2 - \alpha^2}(\rho), \\ \epsilon \mathcal{L}_1(\rho) &= \kappa_1 D_{\hat{a}}(\rho) - i \frac{\pi}{4\alpha T} [\hat{a} + \hat{a}^\dagger, \rho] \end{aligned} \quad (28)$$

where  $\kappa_1/\kappa_2$  and  $T\kappa_2$  are much smaller than 1, ensuring the scaling based on the small parameter  $\epsilon$ . Moreover, replacing  $\mathcal{L}_1$  in formulae (18) and (20) by the superoperator  $\kappa_1 D_{\hat{a}}(\bullet) - i \frac{\pi}{4\alpha T} [\hat{a} + \hat{a}^\dagger, \bullet]$  corresponding to  $\epsilon \mathcal{L}_1$ , provides directly  $\epsilon F_{d',d}^{(1)}$ ,  $\epsilon \hat{S}_d^{(1)}$  and  $\epsilon^2 F_{d',d}^{(2)}$  without defining precisely  $\epsilon$ .

Numerical simulations of figures 1, 2 and 4 are based on a Galerkin approximation of the Hilbert space relying on the photon-number state  $|n\rangle$  with  $n$  between 0 to  $N$ . The integer  $N$  is chosen large enough to ensure that  $|\langle \alpha | N \rangle|^2 = e^{-|\alpha|^2} |\alpha|^{2N}/N!$  remains negligible. The time discretization of the resulting finite-dimensional system of ordinary differential equations is based on the numerical scheme described in appendix C. It provides a discrete-time setting  $\rho(t + \delta t) = \mathcal{K}_0(\rho(t)) + \epsilon \mathcal{K}_1(\rho(t))$  where  $\mathcal{K}_0$  is an exact quantum channel close to identity with

$$\begin{aligned} \kappa_2 \delta t &= \frac{1}{1000}, \quad \kappa_1 = \frac{\kappa_2}{100}, \\ \epsilon_Z &= \frac{\pi}{4\alpha T} = \frac{\kappa_2}{20}, \quad 1 \leq \alpha^2 \leq 16 \text{ and } N = 100. \end{aligned} \quad (29)$$

The operators  $\hat{S}_d^{(0)} = \hat{S}_d$  with  $d = 1, \dots, 4 = \bar{d}$  are obtained from truncated approximations of coherent states  $|\pm\alpha\rangle \approx e^{-\alpha^2/2} \sum_{n=0}^N \frac{(\pm\alpha)^n}{\sqrt{n!}} |n\rangle$ . The associated invariant operators  $\hat{J}_d$  are obtained numerically via the discrete-time formulation given in appendix D. Similarly, the entries of  $\epsilon F_{d',d}^{(1)}$  and  $\epsilon^2 F_{d',d}^{(2)}$  are given by discrete-time formulae (D6) divided by  $\delta t$  and where  $\mathcal{K}_1$  stands for  $\epsilon \delta t \mathcal{L}_1$ . These matrices provide, up to third-order terms, the generator of the continuous-time reduced dynamics:

$$\frac{d}{dt}x = (\epsilon F^{(1)} + \epsilon^2 F^{(2)})x = F(\epsilon)x + O(\epsilon^3) \quad (30)$$

where  $x_d = \text{Tr}(\hat{J}_d \rho)$  for  $d = 1, \dots, 4$ .

On figure 1, the reduced model propagator  $G_{\text{red}} = e^{T(\epsilon F^{(1)} + \epsilon^2 F^{(2)})}$ , a  $4 \times 4$  real matrix, is then compared to the full model propagator  $G_{\text{full}}$ , another  $4 \times 4$  real matrix with entries given by  $\text{Tr}(\hat{J}_{d'} \widehat{W}_d(T))$  where  $\widehat{W}_d(t)$  is the numerical solution of the full model (1) truncated to  $N = 100$  photons and starting from initial condition  $\widehat{W}_d(0) = \hat{S}_d$ . We observe an error  $\sqrt{\text{Tr}((G_{\text{red}} G_{\text{full}}^{-1} - I_4)(G_{\text{red}} G_{\text{full}}^{-1} - I_4)^\dagger)}$  of less than 0.014 for mean-photon number  $\alpha^2$  between 1 and 16 ( $I_4$  is the  $4 \times 4$  identity matrix).

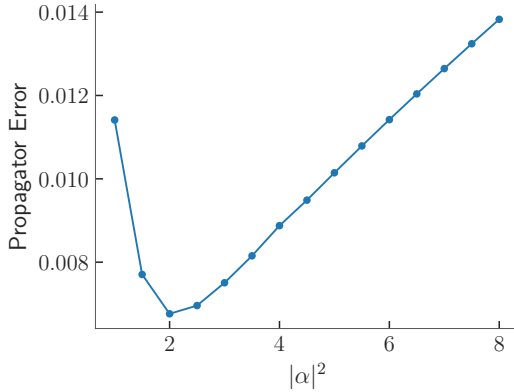


FIG. 1: Propagator error between the full-model (28) and reduced model (30) for the Z gate with the mean photon number  $\alpha^2$  between 1 and 16. The error is computed as  $\sqrt{\text{Tr}((G_{\text{red}} G_{\text{full}}^{-1} - I_4)(G_{\text{red}} G_{\text{full}}^{-1} - I_4)^\dagger)}$ .

Both  $G_{\text{red}}$  and  $G_{\text{full}}$  are close to the ideal Z-gate matrix

$$G_{\text{ideal}} = \begin{pmatrix} 1 & 0 & 0 & 0 \\ 0 & -1 & 0 & 0 \\ 0 & 0 & -1 & 0 \\ 0 & 0 & 0 & 1 \end{pmatrix}.$$

Thus, the reduced model error propagator  $E_{\text{red}} = G_{\text{ideal}}^{-1} G_{\text{red}}$  and the full model error propagator  $E_{\text{full}} = G_{\text{ideal}}^{-1} G_{\text{full}}$  are close to identity matrix  $I_4$ : they correspond in fact to quantum channels usually close to identity and characterizing the errors. These channels can

be decomposed according to the basis  $(\hat{S}_1, \dots, \hat{S}_4)$ . This means that for  $E = E_{\text{red}}, E_{\text{full}}$ , the identity

$$\forall x \in \mathbb{R}^4, \quad \sum_{d,d'=1}^4 E_{d,d'} x_{d'} \hat{S}_d = \sum_{m,n=1}^4 \chi_{m,n}^E \hat{S}_m \left( \sum_{d=1}^4 x_d \hat{S}_d \right) \hat{S}_n \quad (31)$$

uniquely defines the  $\chi^E$  matrix, a  $4 \times 4$ -matrix, characterizing the errors and close to  $\chi^{I_4}$  having a single non-zero entry  $\chi_{1,1}^{I_4} = 1$ . This is illustrated on figure 2.

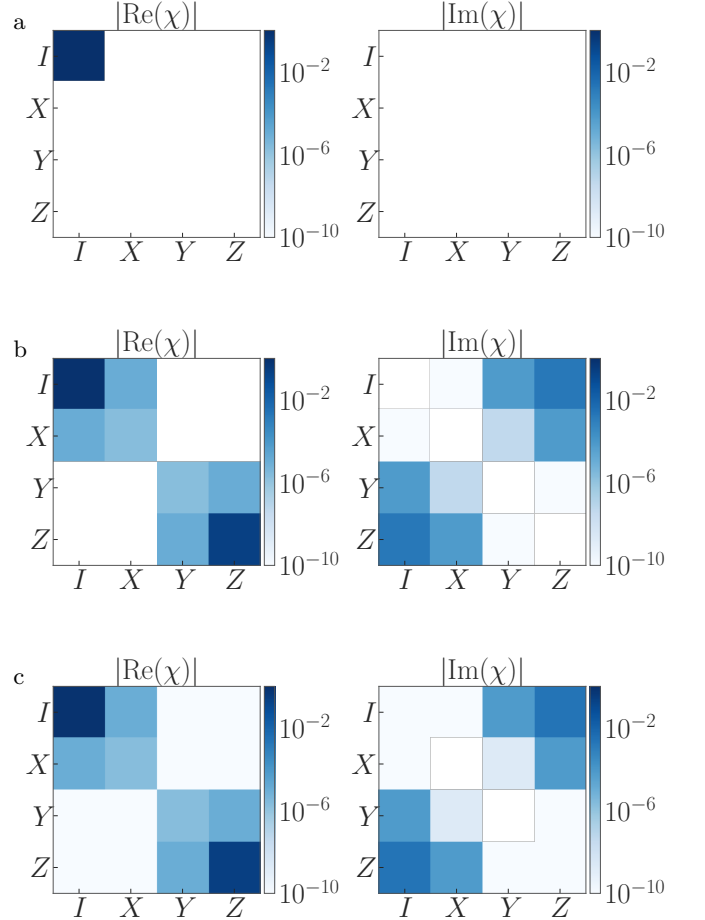


FIG. 2: Real (left) and imaginary (right) part of the quantum-error matrix  $\chi^E$ . (a) corresponds to no-error with  $E = I_4$ ; (b) corresponds to full model simulations (28) with  $\alpha^2 = 4$  and  $E = E_{\text{full}}$ ; (c) corresponds to reduced model simulations (30) with  $\alpha^2 = 4$  and  $E = E_{\text{red}}$ .

Since  $\hat{X} = \sqrt{2}\hat{S}_2$ ,  $\hat{Y} = \sqrt{2}\hat{S}_3$  and  $\hat{Z} = \sqrt{2}\hat{S}_4$  correspond to three Pauli operators on the code-space,  $\chi_{2,2}^E$  (resp.  $\chi_{3,3}^E, \chi_{4,4}^E$ ) gives roughly-speaking the X-error (resp. Y-error, Z-error) probability, see figure 3. These error probabilities have to be less than some thresholds



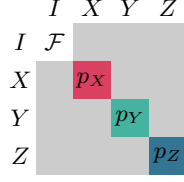


FIG. 3: One-qubit  $\chi$  matrix representing the noise channel of an imperfect gate reduced to a two-level system. The off-diagonal elements shown in gray are ignored since they do not cause symmetric Pauli errors.

in order to be cancelled by high-level error correction code. For cat-qubit, Z-error probability is usually much larger than the two other ones, X-error and Y-error probabilities, called bit-flip errors. Simulations of figure 4a show that the reduced model captures the very small error probabilities associated to bit-flip errors known to be exponentially suppressed for large  $|\alpha|^2$  as shown experimentally in [38]. We found an exponential suppression of bit-flips proportional to  $\exp^{-a|\alpha|^2}$  with  $a = 2.46 \pm 0.03$ . The reduced model also captures the phase-flips (Z-error) in figure 4b. It matches well with full model simulations and also with an analytical formula obtained via a perturbation expansion given in [19]:  $p_Z = |\alpha|^2 \kappa_1 T + \frac{\epsilon_Z^2 T}{|\alpha|^2 \kappa_2}$ .

Z-gate simulations up to order 5 are discussed in appendix A 2, showing the convergence of the X, Y and Z error probabilities by increasing the order of the perturbative analysis in figure 10. The equation (16) allows performing leakage computation, defined as the population outside the code space, see appendix F 1 and figure 16a.

### III. COMPOSITE SYSTEMS AND ZZ/ZZZ-GATE SIMULATIONS

#### A. Second-order approximation with only local computations

Take a bipartite system made of sub-systems  $A$  and  $B$  with Hilbert spaces  $\mathcal{H}_A$  and  $\mathcal{H}_B$ . The system Hilbert space is  $\mathcal{H} = \mathcal{H}_A \otimes \mathcal{H}_B$ . Assume that the unperturbed dynamics  $\mathcal{L}_0$  in (1) admit the following structure:

$$\mathcal{L}_0 = \mathcal{L}_{A,0} + \mathcal{L}_{B,0} \quad (32)$$

where  $\mathcal{D}_{A,0}$  and  $\mathcal{D}_{B,0}$  are the steady-state subspaces of operators on  $\mathcal{H}_A$  and  $\mathcal{H}_B$  of local Lindblad superoperators  $\mathcal{L}_{A,0}$  and  $\mathcal{L}_{B,0}$ . These local nominal dynamics stabilize the subspaces of dimensions  $\bar{d}_A$  and  $\bar{d}_B$ , having  $(\hat{S}_{A,d_A})_{1 \leq d_A \leq \bar{d}_A}$  and  $(\hat{S}_{B,d_B})_{1 \leq d_B \leq \bar{d}_B}$  as orthonormal basis of Hermitian operators. Thus, all Hermitian operators in  $\mathcal{D}_0$ , the kernel of  $\mathcal{L}_A + \mathcal{L}_B$ , read

$$\sum_{d_A, d_B} x_{d_A, d_B} \hat{S}_{A, d_A} \otimes \hat{S}_{B, d_B} \quad (33)$$

where  $x_{d_A, d_B}$  are arbitrary real numbers.

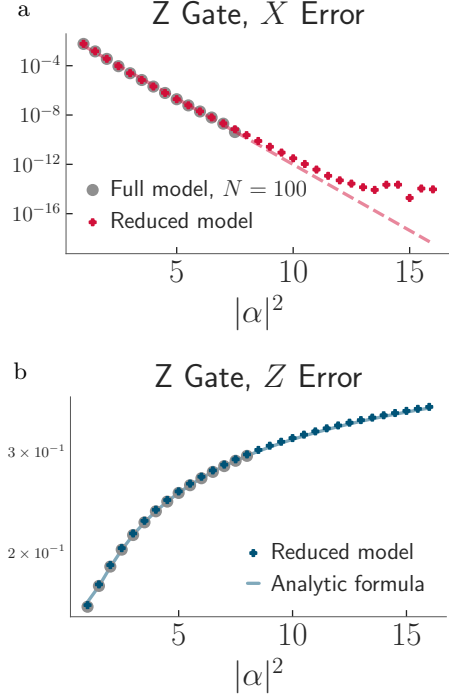


FIG. 4: Comparison between (a) X and (b) Z error probabilities of a Z gate obtained via full model simulations for  $|\alpha|^2 \leq 8$  (28) (shown as gray circles) and the reduced model simulations (30) (colored plus) for different mean photon numbers  $\alpha^2$ . A simple fit yields an exponential suppression of bit-flips with an exponential coefficient of  $2.46 \pm 0.03$  (dashed line).

We assume that  $\mathcal{L}_{A,0}$  and  $\mathcal{L}_{B,0}$  ensure exponential convergence towards  $\mathcal{D}_{A,0}$  and  $\mathcal{D}_{B,0}$ : for any operators  $\rho$  on  $\mathcal{H}$ ,

$$\begin{aligned} \lim_{t \rightarrow +\infty} e^{t(\mathcal{L}_{A,0} + \mathcal{L}_{B,0})}(\rho) &= \bar{\mathcal{K}}_0(\rho) \\ &= \sum_{d_A, d_B} \text{Tr} \left( \hat{J}_{A, d_A} \otimes \hat{J}_{B, d_B} \rho \right) \hat{S}_{A, d_A} \otimes \hat{S}_{B, d_B} \end{aligned} \quad (34)$$

where  $\hat{J}_{A, d_A}$  and  $\hat{J}_{B, d_B}$  are local invariant operators

$$\begin{aligned} \hat{J}_{A, d_A} &= \lim_{t \rightarrow +\infty} e^{t\mathcal{L}_{A,0}^*}(\hat{S}_{A, d_A}), \\ \hat{J}_{B, d_B} &= \lim_{t \rightarrow +\infty} e^{t\mathcal{L}_{B,0}^*}(\hat{S}_{B, d_B}). \end{aligned} \quad (35)$$

Assume that  $\hat{H}_1$  and  $\mathcal{L}_{1,\nu}$  defining the super operator  $\mathcal{L}_1$  in (1) only involve finite sums of tensor products of operators on  $\mathcal{H}_A$  and  $\mathcal{H}_B$ . This means that for any  $\hat{X}_A$  and  $\hat{X}_B$  local operators on  $\mathcal{H}_A$  and  $\mathcal{H}_B$ ,

$$\mathcal{L}_1(\hat{X}_A \otimes \hat{X}_B) = \sum_{\nu=1}^{\bar{\nu}} \hat{L}_{A,\nu} \hat{X}_A \hat{R}_{A,\nu} \otimes \hat{L}_{B,\nu} \hat{X}_B \hat{R}_{B,\nu} \quad (36)$$

where  $\bar{\nu}$  is a positive integer, where  $\hat{L}_{A,\nu}$ ,  $\hat{R}_{A,\nu}$  are operators on  $\mathcal{H}_A$  and where  $\hat{L}_{B,\nu}$ ,  $\hat{R}_{B,\nu}$  are operators on  $\mathcal{H}_B$ .

The operator  $\hat{J}_{d'}$  appearing in (13) corresponds here to  $\hat{J}_{A,d'_A} \otimes \hat{J}_{B,d'_B}$  with  $d' = (d'_A, d'_B)$ . Similarly,  $\hat{S}_d$  reads here  $\hat{S}_{A,d_A} \otimes \hat{S}_{B,d_B}$  with  $d = (d_A, d_B)$ . With (36) one obtains

$$F_{(d'_A, d'_B), (d_A, d_B)}^{(1)} = \sum_{\nu=1}^{\bar{\nu}} \text{Tr} \left( \hat{J}_{A, d'_A} \hat{L}_{A, \nu} \hat{S}_{A, d_A} \hat{R}_{A, \nu} \right) \dots \text{Tr} \left( \hat{J}_{B, d'_B} \hat{L}_{B, \nu} \hat{S}_{B, d_B} \hat{R}_{B, \nu} \right). \quad (37)$$

For  $X = A, B$ , consider the local operators

$$\hat{J}_{X, d'_X, \nu} = \hat{R}_{X, \nu} \hat{J}_{X, d'_X} \hat{L}_{X, \nu}, \quad \hat{S}_{X, d_X, \nu} = \hat{L}_{X, \nu} \hat{S}_{X, d_X} \hat{R}_{X, \nu}. \quad (38)$$

Then

$$\begin{aligned} F_{(d'_A, d'_B), (d_A, d_B)}^{(1)} &= \sum_{\nu=1}^{\bar{\nu}} \text{Tr} \left( \hat{J}_{A, d'_A} \hat{S}_{A, d_A, \nu} \right) \text{Tr} \left( \hat{J}_{B, d'_B} \hat{S}_{B, d_B, \nu} \right) \\ &= \sum_{\nu=1}^{\bar{\nu}} \text{Tr} \left( \hat{S}_{A, d_A} \hat{J}_{A, d'_A, \nu} \right) \text{Tr} \left( \hat{S}_{B, d_B} \hat{J}_{B, d'_B, \nu} \right). \end{aligned} \quad (39)$$

This gives the first-order approximation of the reduced dynamics for which the coordinate vector  $x =$

$(x_{d'_A, d'_B})_{d'_A, d'_B}$  evolves according to:

$$\frac{d}{dt} x_{d'_A, d'_B} = \sum_{d_A, d_B} \epsilon F_{(d'_A, d'_B), (d_A, d_B)}^{(1)} x_{d_A, d_B}. \quad (40)$$

Take the second-order correction  $F^{(2)}$  given by the general formula (20). We have

$$\begin{aligned} \mathcal{L}_1^*(\hat{J}_{d'}) &= \sum_{\nu'=1}^{\bar{\nu}} \hat{J}_{A, d'_A, \nu'} \otimes \hat{J}_{B, d'_B, \nu'}, \\ \mathcal{L}_1(\hat{S}_d) &= \sum_{\nu=1}^{\bar{\nu}} \hat{S}_{A, d_A, \nu} \otimes \hat{S}_{B, d_B, \nu} \end{aligned} \quad (41)$$

where  $d' = (d'_A, d'_B)$  and  $d = (d_A, d_B)$ . By linearity of  $\bar{\mathcal{R}}_0$

$$\begin{aligned} \mathcal{L}_1^*(\hat{J}_{d'}) \bar{\mathcal{R}}_0(\mathcal{L}_1(\hat{S}_d)) &= \sum_{\nu, \nu'=1}^{\bar{\nu}} \left( \hat{J}_{A, d'_A, \nu'} \otimes \hat{J}_{B, d'_B, \nu'} \right) \bar{\mathcal{R}}_0 \left( \hat{S}_{A, d_A, \nu} \otimes \hat{S}_{B, d_B, \nu} \right). \end{aligned} \quad (42)$$

Combining  $e^{s\mathcal{L}_{A,0} + s\mathcal{L}_{B,0}} = e^{s\mathcal{L}_{A,0}} \otimes e^{s\mathcal{L}_{B,0}}$  with (17) and (34) gives

$$\begin{aligned} \bar{\mathcal{R}}_0 \left( \hat{S}_{A, d_A, \nu} \otimes \hat{S}_{B, d_B, \nu} \right) &= \int_0^{+\infty} \left( e^{s\mathcal{L}_{A,0}} \left( \hat{S}_{A, d_A, \nu} \right) \otimes e^{s\mathcal{L}_{B,0}} \left( \hat{S}_{B, d_B, \nu} \right) \right. \\ &\quad \left. - \sum_{d''_A, d''_B} \text{Tr} \left( \hat{J}_{A, d'_A} \hat{S}_{A, d_A, \nu} \right) \text{Tr} \left( \hat{J}_{B, d'_B} \hat{S}_{B, d_B, \nu} \right) \hat{S}_{A, d''_A} \otimes \hat{S}_{B, d''_B} \right) ds \end{aligned} \quad (43)$$

Here, we are only interested in the trace of the product with  $\hat{J}_{A, d'_A, \nu'} \otimes \hat{J}_{B, d'_B, \nu'}$ :

$$\begin{aligned} &\text{Tr} \left( \hat{J}_{A, d'_A, \nu'} \otimes \hat{J}_{B, d'_B, \nu'} \bar{\mathcal{R}}_0 \left( \hat{S}_{A, d_A, \nu} \otimes \hat{S}_{B, d_B, \nu} \right) \right) \\ &= \int_0^{+\infty} \left( \text{Tr} \left( \hat{J}_{A, d'_A, \nu'} e^{s\mathcal{L}_{A,0}} \left( \hat{S}_{A, d_A, \nu} \right) \right) \text{Tr} \left( \hat{J}_{B, d'_B, \nu'} e^{s\mathcal{L}_{B,0}} \left( \hat{S}_{B, d_B, \nu} \right) \right) \dots \right. \\ &\quad \left. \dots - \sum_{d''_A, d''_B} \text{Tr} \left( \hat{J}_{A, d'_A} \hat{S}_{A, d_A, \nu} \right) \text{Tr} \left( \hat{J}_{B, d'_B} \hat{S}_{B, d_B, \nu} \right) \text{Tr} \left( \hat{J}_{A, d'_A, \nu'} \hat{S}_{A, d''_A} \right) \text{Tr} \left( \hat{J}_{B, d'_B, \nu'} \hat{S}_{B, d''_B} \right) \right) ds \\ &= \int_0^{+\infty} \left( \text{Tr} \left( \hat{J}_{A, d'_A, \nu'} e^{s\mathcal{L}_{A,0}} \left( \hat{S}_{A, d_A, \nu} \right) \right) \text{Tr} \left( \hat{J}_{B, d'_B, \nu'} e^{s\mathcal{L}_{B,0}} \left( \hat{S}_{B, d_B, \nu} \right) \right) \dots \right. \\ &\quad \left. \dots - G_{A, d'_A, d_A, \nu, \nu'} G_{B, d'_B, d_B, \nu, \nu'} \right) ds, \end{aligned}$$

where for  $X = A, B$

$$\begin{aligned} G_{X, d'_X, d_X, \nu, \nu'} &= \sum_{d''_X} \text{Tr} \left( \hat{J}_{X, d'_X} \hat{S}_{X, d''_X, \nu'} \right) \text{Tr} \left( \hat{J}_{X, d'_X} \hat{S}_{X, d_X, \nu} \right) \end{aligned}$$

and using identities like  $\text{Tr}(\hat{J}_{X,d'_X} \hat{S}_{X,d''_X,\nu'}) \equiv \text{Tr}(\hat{S}_{X,d''_X} \hat{J}_{X,d'_X,\nu'})$ .

To conclude, one gets each entry of  $F^{(2)}$  with only local numerical computations on  $\mathcal{H}_A$  and  $\mathcal{H}_B$ :

$$F_{(d'_A,d'_B),(d_A,d_B)}^{(2)} = \sum_{\nu,\nu'=1}^{\bar{\nu}} \int_0^{+\infty} \left( \text{Tr}(\hat{J}_{A,d'_A,\nu'} e^{s\mathcal{L}_{A,0}}(\hat{S}_{A,d_A,\nu})) \text{Tr}(\hat{J}_{B,d'_B,\nu'} e^{s\mathcal{L}_{B,0}}(\hat{S}_{B,d_B,\nu})) \dots \right. \\ \left. \dots - G_{A,d'_A,d_A,\nu,\nu'} G_{B,d'_B,d_B,\nu,\nu'} \right) ds. \quad (44)$$

The equivalent of Eqs. (39) and (44) for a discrete time setting are given in appendix D 2.

### B. ZZ gate

A ZZ-gate corresponds to a unitary transformation changing  $|\mathcal{C}_\alpha^\pm\rangle |\mathcal{C}_\alpha^\pm\rangle$  to  $|\mathcal{C}_\alpha^\mp\rangle |\mathcal{C}_\alpha^\mp\rangle$  (parity change). As for the Z-gate implementation, it can be approximately engineered via the propagator of time duration  $T > 0$  associated to the Hamiltonian  $\hat{H}_1 = \epsilon_{ZZ} (\hat{a}\hat{b}^\dagger + \hat{a}^\dagger\hat{b})$  where  $\hat{a}$  (resp.  $\hat{b}$ ) is the photon annihilation operator on subsystem  $A$  (resp.  $B$ ) and where  $\epsilon_{ZZ} = \frac{\pi}{4\alpha^2 T}$  has to be much smaller than  $\kappa_2$ . The superoperators  $\mathcal{L}_0$  and  $\mathcal{L}_1$  corresponding here to Eq. (1) are thus

$$\mathcal{L}_0(\rho) = \kappa_2 \left[ D_{\hat{a}^2 - \alpha^2} + D_{\hat{b}^2 - \alpha^2} \right] (\rho), \\ \epsilon \mathcal{L}_1(\rho) = \kappa_1 \left[ D_{\hat{a}} + D_{\hat{b}} \right] (\rho) - i \frac{\pi}{4\alpha^2 T} \left[ (\hat{a}\hat{b}^\dagger + \hat{a}^\dagger\hat{b}) \cdot \rho \right] \quad (45)$$

where  $\kappa_1/\kappa_2$  and  $T\kappa_2$  are much smaller than 1.

$\epsilon F_{(d'_A,d'_B),(d_A,d_B)}^{(1)}$  and  $\epsilon^2 F_{(d'_A,d'_B),(d_A,d_B)}^{(2)}$  defined in (39) and (44) are computed using discrete-time formulae and

provide, up to third-order terms, the generator of the continuous-time reduced dynamics of Eq. (30) with the coordinate-vector  $x$

$$x = \left( x_{(d_A,d_B)} = \text{Tr}(\hat{J}_{d_A} \otimes \hat{J}_{d_B} \rho) \right)_{d_A,d_B=1,\dots,4}.$$

The parameters of the numerical simulations of figures 6 are

$$\kappa_2 \delta t = \frac{1}{1000}, \quad \kappa_1 = \frac{\kappa_2}{100}, \\ \epsilon_{ZZ} = \frac{\pi}{4\alpha^2 T} = \frac{\kappa_2}{20} \text{ with } 1 \leq \alpha^2 \leq 16$$

where photon-number truncation  $N$  is equal to 100 for the reduced-model and to 40 for the full-model.

As for the Z gate, the reduced model error propagator  $E_{\text{red}} = G_{\text{ideal}}^{-1} G_{\text{red}}$  and the full model error propagator  $E_{\text{full}} = G_{\text{ideal}}^{-1} G_{\text{full}}$  are close to identity matrix  $I_{16}$  and characterize the errors. These channels can also be decomposed according to the basis  $(\hat{S}_{A,1}, \dots, \hat{S}_{A,4}) \otimes (\hat{S}_{B,1}, \dots, \hat{S}_{B,4})$ . This means that for  $E = E_{\text{red}}, E_{\text{full}}$ , the following identity

$$\forall x \in \mathbb{R}^{16}, \quad \sum_{d_A,d_B,d'_A,d'_B=1}^4 E_{(d_A,d_B),(d'_A,d'_B)} x_{(d'_A,d'_B)} \hat{S}_{A,d_A} \hat{S}_{B,d_B} \\ = \sum_{m_A,m_B,n_A,n_B=1}^4 \chi_{(m_A,m_B),(n_A,n_B)}^E \hat{S}_{A,m_A} \hat{S}_{B,m_B} \left( \sum_{d_A,d_B=1}^4 x_{(d_A,d_B)} \hat{S}_{A,d_A} \hat{S}_{B,d_B} \right) \hat{S}_{A,n_A} \hat{S}_{B,n_B} \quad (46)$$

uniquely defines the  $16 \times 16$ ,  $\chi^E$  matrix characterizing the errors (close to  $\chi^{I_{16}}$  having a single non-zero entry  $\chi_{1,1}^{I_{16}} = 1$ ). An illustration of  $\chi^{E_{\text{red}}}$  and  $\chi^{E_{\text{full}}}$  is given in appendix E, figure 12 for  $\alpha = 2$ .

Coefficients of the diagonal of  $\chi^E$  give the Pauli errors of the gate. In figure 5, the total bit-flip error probability is displayed as the sum of all the 12 Pauli errors involving a bit flip ( $X$ - or  $Y$ -error) and simulated in figure 6a. We



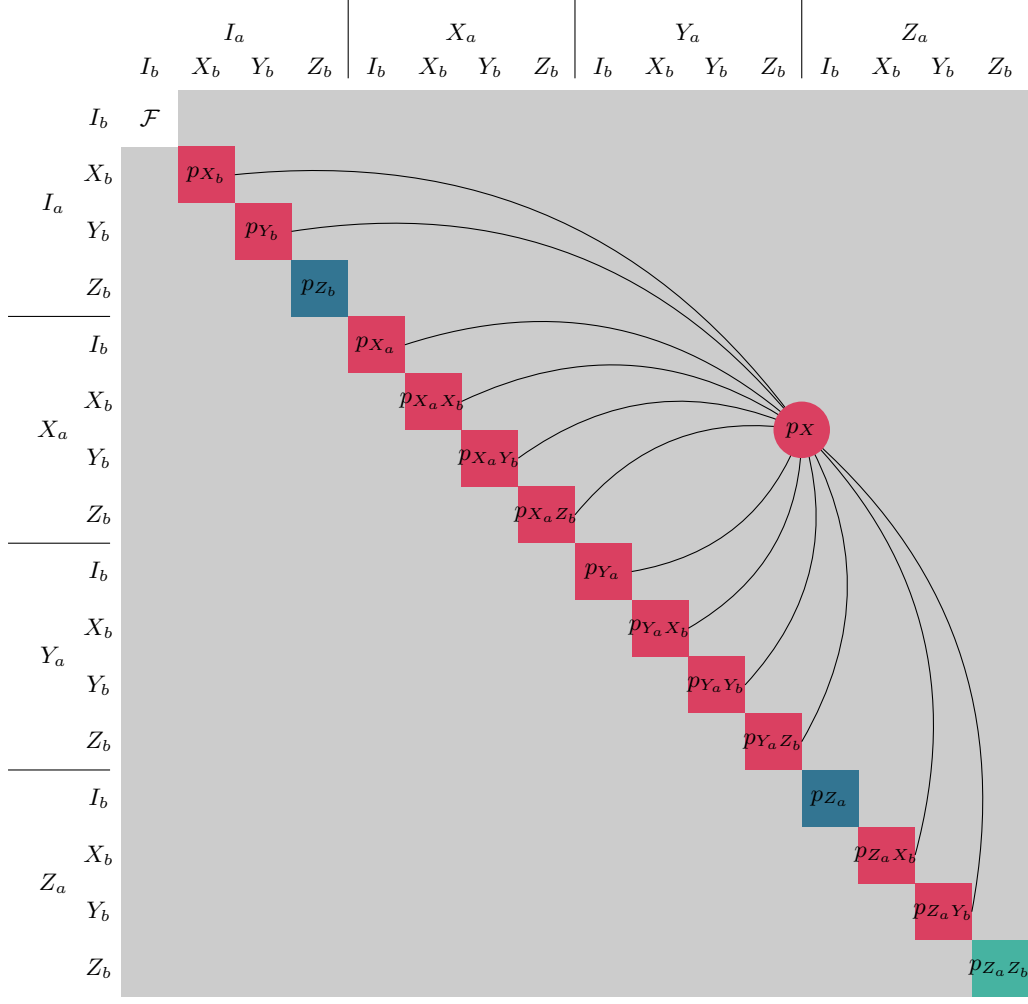


FIG. 5: Two-qubit  $\chi$  matrix representing the noise channel of an imperfect gate reduced to two two-level systems. The off-diagonal elements shown in gray are not considered in such a rough analysis based on symmetric Pauli errors.

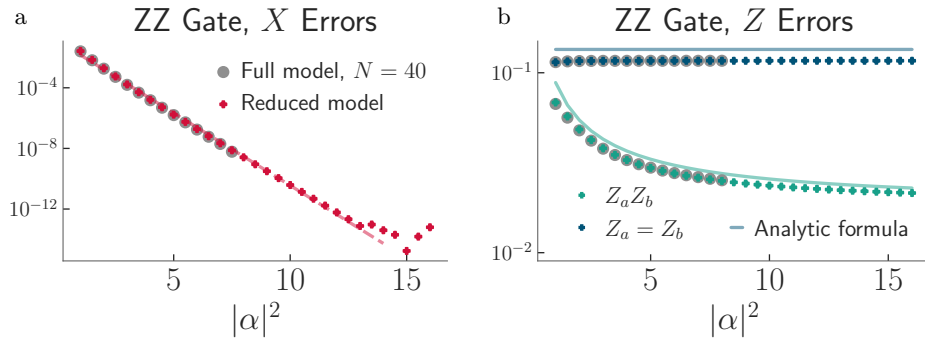


FIG. 6: Comparison between (a)  $X$  and (b)  $Z$  error probabilities of a  $ZZ$  gate,  $p_{ZZ}$  in green and  $p_Z$  in blue, obtained via full model simulations for  $|\alpha|^2 \leq 8$  (45) (shown as gray circles) and the reduced model simulations (30) (colored plus) for different mean photon numbers  $|\alpha|^2$ . A simple fit yields an exponential suppression of bit-flips with an exponential coefficient of  $2.20 \pm 0.01$  (dashed line).

found an exponential suppression of bit flips proportional to  $\exp^{-a|\alpha|^2}$  with  $a = 2.20 \pm 0.01$ . The reduced model also captures the phase flips (Z-error) in figure 6b. It matches well with full-model simulations and also with an analytical formula obtained via a perturbation expansion derived from the formula of the Z-gate errors:  $p_{Z_a} = p_{Z_b} = |\alpha|^2 \kappa_1 T = \frac{\pi \kappa_1}{4\epsilon_{ZZ}}, p_{Z_a Z_b} = \frac{\pi \epsilon_{ZZ}}{2|\alpha|^4 \kappa_2} + p_{Z_a} p_{Z_b}$  (the last term coming from second-order effects of the single photon losses), see appendix G.

The equation (16) allows to perform a first-order computation of the leakage, see appendix F 2 and figure 16b.

### C. ZZZ gate

A ZZZ-gate unitary corresponds to a transformation changing  $|\mathcal{C}_\alpha^\pm\rangle |\mathcal{C}_\alpha^\pm\rangle |\mathcal{C}_\alpha^\pm\rangle$  to  $|\mathcal{C}_\alpha^\mp\rangle |\mathcal{C}_\alpha^\mp\rangle |\mathcal{C}_\alpha^\mp\rangle$ . As for the Z- and ZZ-gate, it can be approximately engineered via the propagator of time duration  $T > 0$  associated to the Hamiltonian  $\hat{H}_1 = \epsilon_{ZZZ} (\hat{a}\hat{b}\hat{c}^\dagger + \hat{a}^\dagger\hat{b}^\dagger\hat{c})$  where  $\hat{a}$  (resp.  $\hat{b}, \hat{c}$ ) is the photon annihilation operator on sub-system  $A$  (resp.  $B, C$ ) and where  $\epsilon_{ZZZ} = \frac{\pi}{4\alpha^3 T}$  has to be much smaller than  $\kappa_2$ . The superoperators  $\mathcal{L}_0$  and  $\mathcal{L}_1$  corresponding here to Eq. (1) are thus

$$\begin{aligned} \mathcal{L}_0(\rho) &= \kappa_2 \left[ D_{\hat{a}^2 - \alpha^2} + D_{\hat{b}^2 - \alpha^2} + D_{\hat{c}^2 - \alpha^2} \right] (\rho), \\ \epsilon \mathcal{L}_1(\rho) &= \kappa_1 \left[ D_{\hat{a}} + D_{\hat{b}} + D_{\hat{c}} \right] (\rho) \\ &\quad - i \frac{\pi}{4\alpha^3 T} \left[ (\hat{a}\hat{b}\hat{c}^\dagger + \hat{a}^\dagger\hat{b}^\dagger\hat{c}), \rho \right] \end{aligned} \quad (47)$$

where  $\kappa_1/\kappa_2$  and  $T\kappa_2$  are much smaller than 1.

Numerical simulations of the full-model were not performed for computational limitations. We only report reduced-model simulations based on the direct generalization of (39) and (44) to a tripartite system. The parameters of the numerical simulations of figures 7 are

$$\begin{aligned} \kappa_2 \delta t &= \frac{1}{1000}, \quad \kappa_1 = \frac{\kappa_2}{100}, \\ \epsilon_{ZZZ} &= \frac{\pi}{4\alpha^2 T} = \frac{\kappa_2}{20} \text{ with } 1 \leq \alpha^2 \leq 16, \quad N = 100. \end{aligned}$$

The total bit-flip error probability is the sum of all the 56 Pauli errors involving a bit flip ( $X$ - or  $Y$ -error) and simulated in figure 7a. We found an exponential suppression of bit flips proportional to  $\exp^{-a|\alpha|^2}$  with  $a = 2.12 \pm 0.01$ . The reduced model also captures the phase flips (Z-error) in figure 7b. It matches well with an analytical formula obtained via a perturbation expansion detailed in appendix G:  $p_{Z_a} =$

$p_{Z_b} = p_{Z_c} = |\alpha|^2 \kappa_1 T = \frac{\pi \kappa_1}{4|\alpha| \epsilon_{ZZZ}}, p_{Z_a Z_b Z_c} = \frac{3\pi \epsilon_{ZZZ}}{4|\alpha| \kappa_2} + p_{Z_a} p_{Z_b} p_{Z_c}, p_{Z_a Z_b} = p_{Z_a Z_c} = p_{Z_b Z_c} = p_{ZZ} p_{ZZZ} + p_{ZZ}^2$ . An illustration of  $64 \times 64 \chi^E$  matrix for the reduced propagator error  $E_{\text{red}}$  is given in appendix E, figure 13. A first-order computation of the leakage is shown in figure 16c.

## IV. COMPOSITE SYSTEMS WITH AN UNSTABILIZED COMPONENT

### A. Second-order approximation

Assume that  $\mathcal{L}_{B,0} = 0$  for the bipartite system of section III. Then  $(\hat{S}_{B,d_B})_{1 \leq d_B \leq \bar{d}_B}$  span all Hermitian operators on  $\mathcal{H}_B$  and  $\hat{J}_{B,d_B} = \hat{S}_{B,d_B}$ . Following (33), all operators belonging to  $\mathcal{D}_0$  read  $\sum_{d_A} \hat{S}_{A,d_A} \otimes \rho_{B,d_A}$  with hermitian operators on  $\mathcal{H}_B$

$$\rho_{B,d_A} = \sum_{d_B} x_{d_A d_B} \hat{S}_{B,d_B} \quad (48)$$

and  $x_{d_A, d_B} = \text{Tr}(\hat{S}_{B,d_B} \rho_{B,d_A})$  real numbers. The mapping between  $x = (x_{d_A, d_B})$  and the set  $(\rho_{B,d_A})$  of  $\bar{d}_A$  operators on  $\mathcal{H}_B$  is linear and bijective. We just translate here the formulae of section III with  $x_{d_A, d_B}$  variables in  $\rho_{B,d_A}$  variables.

Combining (39) with (40), the first-order time evolution of the coordinate vector  $(x_{d'_A, d'_B})_{d'_A, d'_B}$  reads

$$\begin{aligned} \frac{d}{dt} x_{d'_A, d'_B} &= \sum_{\nu, d_A, d_B} \text{Tr}(\hat{J}_{A, d'_A} \hat{L}_{A, \nu} \hat{S}_{A, d_A} \hat{R}_{A, \nu}) \dots \\ &\quad \dots \text{Tr}(\hat{S}_{B, d'_B} \hat{L}_{B, \nu} \hat{S}_{B, d_B} \hat{R}_{B, \nu}) x_{d_A, d_B}. \end{aligned}$$

Using (48), we get

$$\frac{d}{dt} \rho_{B, d'_A} = \sum_{\nu, d_A} \text{Tr}(\hat{J}_{A, d'_A} \hat{L}_{A, \nu} \hat{S}_{A, d_A} \hat{R}_{A, \nu}) \hat{L}_{B, \nu} \rho_{B, d_A} \hat{R}_{B, \nu}.$$

With  $\bar{F}_{d'_A, d_A, \nu}^{(1)} = \text{Tr}(\hat{J}_{A, d'_A} \hat{L}_{A, \nu} \hat{S}_{A, d_A} \hat{R}_{A, \nu})$ , the first-order approximation of the slow dynamics reads

$$\frac{d}{dt} \rho_{B, d'_A} = \sum_{\nu, d_A} \bar{F}_{d'_A, d_A, \nu}^{(1)} \hat{L}_{B, \nu} \rho_{B, d_A} \hat{R}_{B, \nu}$$

Using in (38), the superoperator  $\bar{\mathcal{R}}_0$  reads

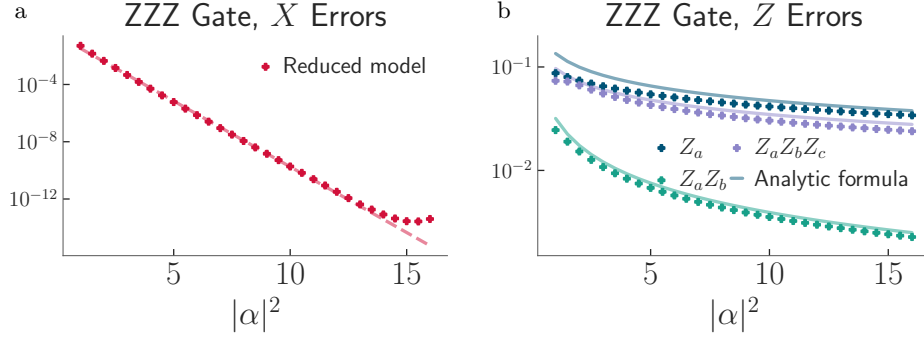


FIG. 7: Comparison between (a)  $X$  and (b)  $Z$  error probabilities of a ZZZ gate,  $p_Z$  ( $p_{Z_a} = p_{Z_b} = p_{Z_c}$ ) in blue,  $p_{ZZ}$  ( $p_{Z_a Z_b} = p_{Z_a Z_c} = p_{Z_b Z_c}$ ) in green and  $p_{Z_a Z_b Z_c}$  in lavender, obtained via reduced model simulations (30) (colored plus) for different mean photon numbers  $|\alpha|^2$ . A simple fit yields an exponential suppression of bit-flips with an exponential coefficient of  $2.12 \pm 0.01$  (dashed line).

$$\begin{aligned}
& \bar{\mathcal{R}}_0(\hat{S}_{A,d_A,\nu} \otimes \hat{S}_{B,d_B,\nu}) \\
&= \int_0^{+\infty} \left( e^{s\mathcal{L}_{A,0}}(\hat{S}_{A,d_A,\nu}) \otimes \hat{S}_{B,d_B,\nu} - \sum_{d''_A, d''_B} \text{Tr}(\hat{J}_{A,d'_A} \hat{S}_{A,d_A,\nu}) \text{Tr}(\hat{S}_{B,d'_B} \hat{S}_{B,d_B,\nu}) \hat{S}_{A,d''_A} \otimes \hat{S}_{B,d''_B} \right) ds \\
&= \int_0^{+\infty} \left( e^{s\mathcal{L}_{A,0}}(\hat{S}_{A,d_A,\nu}) - \sum_{d''_A} \text{Tr}(\hat{J}_{A,d'_A} \hat{S}_{A,d_A,\nu}) \hat{S}_{A,d''_A} \right) ds \otimes \hat{S}_{B,d_B,\nu} \\
&= \bar{\mathcal{R}}_0(\hat{S}_{A,d_A,\nu}) \otimes \hat{S}_{B,d_B,\nu}.
\end{aligned}$$

$\bar{\mathcal{R}}_0$  is thus local on subsystem A.  $F^{(2)}$  given by the formula (44) becomes then

$$\begin{aligned}
F_{(d'_A, d'_B), (d_A, d_B)}^{(2)} &= \text{Tr} \left( \mathcal{L}_1^*(\hat{J}_{A,d'_A} \otimes \hat{S}_{B,d'_B}) \bar{\mathcal{R}}_0(\mathcal{L}_1(\hat{S}_{A,d_A} \otimes \hat{S}_{B,d_B})) \right) \\
&= \sum_{\nu, \nu'} \bar{F}_{d'_A, d_A, \nu, \nu'}^{(2)} \text{Tr}(\hat{S}_{B,d'_B} \hat{L}_{B,\nu'} \hat{L}_{B,\nu} \hat{S}_{B,d_B} \hat{R}_{B,\nu} \hat{R}_{B,\nu'})
\end{aligned}$$

where  $\bar{F}_{d'_A, d_A, \nu, \nu'}^{(2)} = \text{Tr}(\hat{J}_{d'_A, \nu'} \bar{\mathcal{R}}_0(\hat{S}_{d_A, \nu}))$ . With

$$\sum_{d_A, d_B} F_{(d'_A, d'_B), (d_A, d_B)}^{(2)} x_{d_A, d_B} = \sum_{d_A, d_B, \nu, \nu'} \bar{F}_{d'_A, d_A, \nu, \nu'}^{(2)} x_{d_A, d_B} \text{Tr}(\hat{S}_{B,d'_B} \hat{L}_{B,\nu'} \hat{L}_{B,\nu} \hat{S}_{B,d_B} \hat{R}_{B,\nu} \hat{R}_{B,\nu'})$$

and

$$\sum_{d_B} x_{d_A, d_B} \text{Tr}(\hat{S}_{B,d'_B} \hat{L}_{B,\nu'} \hat{L}_{B,\nu} \hat{S}_{B,d_B} \hat{R}_{B,\nu} \hat{R}_{B,\nu'}) = \text{Tr}(\hat{S}_{B,d'_B} \hat{L}_{B,\nu'} \hat{L}_{B,\nu} \rho_{B,d_A} \hat{R}_{B,\nu} \hat{R}_{B,\nu'})$$

we get the following expression for the second-order approximation using the parametrization based on the  $\bar{d}_A$  set of Hermitian operators ( $\rho_{B,d'_A}$ ) on  $\mathcal{H}_B$ :

$$\frac{d}{dt} \rho_{B,d'_A} = \sum_{\nu, d_A} \bar{F}_{d'_A, d_A, \nu}^{(1)} \hat{L}_{B,\nu} \rho_{B,d_A} \hat{R}_{B,\nu} + \sum_{\nu, \nu', d_A} \bar{F}_{d'_A, d_A, \nu, \nu'}^{(2)} \hat{L}_{B,\nu} \hat{L}_{B,\nu'} \rho_{B,d_A} \hat{R}_{B,\nu} \hat{R}_{B,\nu'}. \quad (49)$$

with  $\bar{F}_{d'_A, d_A, \nu}^{(1)} = \text{Tr}(\hat{J}_{A,d'_A} \hat{L}_{A,\nu} \hat{S}_{A,d_A} \hat{R}_{A,\nu})$  and  $\bar{F}_{d'_A, d_A, \nu, \nu'}^{(2)} = \text{Tr}(\hat{J}_{d'_A, \nu'} \bar{\mathcal{R}}_0(\hat{S}_{d_A, \nu}))$ . The discrete-

time formulations of  $\bar{F}_{d'_A, d_A, \nu}^{(1)}$  and  $\bar{F}_{d'_A, d_A, \nu, \nu'}^{(2)}$  can be obtained directly from appendix D 2.

### B. CNOT gate

A CNOT-gate corresponds to a  $\pi$ -rotation in the phase space of a qubit called the target qubit conditioned on the state of another qubit called the control qubit, being on the  $|1\rangle_C \simeq |-\alpha\rangle$  state. Using cat-qubits of complex amplitude  $\alpha$  with  $|\alpha|^2 \gg 1$ , it can be approximately engineered by stabilizing the control cat-qubit via two-photon dissipation and adding the Hamiltonian  $\hat{H}_1 = \frac{\pi}{4\alpha T} (\hat{a} + \hat{a}^\dagger - 2|\alpha|) (\hat{b}^\dagger \hat{b} - |\alpha|^2)$  where  $\hat{a}$  (resp.  $\hat{b}$ ) is the photon annihilation operator on the control cat-qubit  $A$  (resp. the target cat-qubit  $B$ ) and where  $T$  is the gate time.

The original implementation of the CNOT gate [18, 19] includes the target-qubit stabilization via a non local time-varying two-photon dissipation. This implementation is experimentally difficult. Thus, we consider here an easier one with only  $\hat{H}_1$ . This corresponds to a "stroboscopic stabilization" where the target-qubit is stabilized before and after the gate. The simulations below indicate that the exponential suppression of bit flips remains satisfied.

The superoperators  $\mathcal{L}_0$  and  $\mathcal{L}_1$  corresponding here to (1) are thus

$$\begin{aligned} \mathcal{L}_0(\rho) &= \kappa_2 D_{\hat{a}^2 - \alpha^2}(\rho), \\ \epsilon \mathcal{L}_1(\rho) &= \kappa_1 \left[ D_{\hat{a}} + D_{\hat{b}} \right](\rho) \\ &\quad - i \frac{\pi}{4\alpha T} \left[ (\hat{a} + \hat{a}^\dagger - 2|\alpha|) (\hat{b}^\dagger \hat{b} - |\alpha|^2), \rho \right] \end{aligned} \quad (50)$$

where  $\kappa_1/\kappa_2$  and  $\frac{\pi}{4\alpha\kappa_2 T}$  are much smaller than 1.

The complex coefficients  $F_{d'_A, d_A, \nu}^{(1)}$  and  $\bar{F}_{d'_A, d_A, \nu, \nu'}^{(2)}$  of (49) are computed using the discrete-time formulation of appendix D 2 with the following parameters

$$\begin{aligned} \kappa_2 \alpha^2 \delta t &= \frac{1}{1000}, \quad \kappa_1 = \frac{\kappa_2}{100}, \\ T &= \frac{1}{\kappa_2} \text{ with } 1 \leq \alpha^2 \leq 16, \\ N(\alpha) &= \max(20, \lfloor \alpha^2 + 20\alpha \rfloor) \end{aligned}$$

where  $\lfloor \cdot \rfloor$  denotes the integer part. Figures 8 are based on the numerical integration via an explicit Euler scheme of (49), a linear system coupling  $\bar{d}_A = 4$  Hermitian operators on  $\mathcal{H}_B$ :  $(\rho_{B,1}, \dots, \rho_{B,4})$ .

As for the ZZ-gate simulation, the total bit-flip error probability is the sum of all the 12 Pauli errors involving a bit flip ( $X$ - or  $Y$ -error) and corresponds in figure 8a. We found an exponential suppression of bit flips proportional to  $\exp^{-a|\alpha|^2}$  with  $a = 2.204 \pm 0.009$ . The reduced model also captures the phase flips ( $Z$ -error) as illustrated in figure 8b. It matches well with full-model simulations that have been performed for  $|\alpha|^2 \leq 8$ . An illustration of

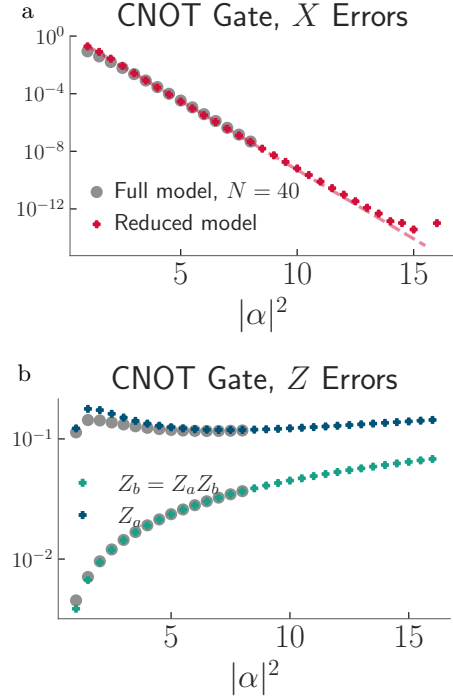


FIG. 8: Comparison between (a)  $X$  and (b)  $Z$  error probabilities of a CNOT gate,  $p_{Z_a Z_b} = p_{Z_b}$  in green and  $p_{Z_a}$  in blue, obtained via full model simulations for  $|\alpha|^2 \leq 8$  (50) (shown as gray circles) and the reduced model simulations (49) (colored plus) for different mean photon numbers  $\alpha^2$ . A simple fit yields an exponential suppression of bit-flips with an exponential coefficient of  $2.204 \pm 0.009$  (dashed line).

$16 \times 16$   $\chi^E$  matrix for the reduced propagator error  $E_{\text{red}}$  and the full propagator error  $E_{\text{full}}$  is given in appendix E, figure 14. A first-order computation of the leakage is shown in appendix F 3 and figure 17a.

### C. CCNOT gate

A CCNOT-gate (Toffoli gate) corresponds to a  $\pi$ -rotation in the phase space of a target qubit conditioned on the state of two control qubits being on the  $|1\rangle_C |1\rangle_C \simeq |-\alpha\rangle |-\alpha\rangle$  state. When  $|\alpha|^2 \gg 1$ , it can be approximately engineered by stabilizing the two control cat-qubits via two-photon dissipation and adding the Hamiltonian  $\hat{H}_1 = -\frac{\pi}{8\alpha^2 T} \left( (\hat{a} - |\alpha|) (\hat{b} - |\alpha|) + \text{h.c.} \right) (\hat{c}^\dagger \hat{c} - |\alpha|^2)$  where  $\hat{a}$  (resp.  $\hat{b}$ ,  $\hat{c}$ ) is the photon annihilation operator on sub-system  $A$  (resp.  $B$ ,  $C$ ) and where  $T$  is the gate time. The superoperators  $\mathcal{L}_0$  and  $\mathcal{L}_1$  corresponding

here to Eq. (1) are thus

$$\begin{aligned}\mathcal{L}_0(\rho) &= \kappa_2 \left[ D_{\hat{a}^2 - \alpha^2} + D_{\hat{b}^2 - \alpha^2} \right] (\rho), \\ \epsilon \mathcal{L}_1(\rho) &= \kappa_1 \left[ D_{\hat{a}} + D_{\hat{b}} + D_{\hat{c}} \right] (\rho) \\ &+ i \frac{\pi}{8\alpha^2 T} \left[ \left( (\hat{a} - |\alpha|) (\hat{b} - |\alpha|) + \text{h.c.} \right) (\hat{c}^\dagger \hat{c} - |\alpha|^2), \rho \right]\end{aligned}\quad (51)$$

where  $\kappa_1/\kappa_2$  and  $\frac{\pi}{8\alpha^2\kappa_2 T}$  are much smaller than 1.

Numerical simulations of the full-model have not been done because of computational limitation. We only report here simulations based on the direct generalisation of (49) to a tripartite system where components one and two are stabilized whereas the third one is not. The parameters of the numerical simulations of figures 9 are

$$\begin{aligned}\kappa_2 \alpha^2 \delta t &= \frac{1}{1000}, \quad \kappa_1 = \frac{\kappa_2}{100}, \\ T &= \frac{1}{\kappa_2} \text{ with } 1 \leq \alpha^2 \leq 16, \\ N(\alpha) &= \max(20, \lfloor \alpha^2 + 20\alpha \rfloor)\end{aligned}$$

where  $\lfloor \cdot \rfloor$  denotes the integer part.

As for the ZZZ-gate simulations, the total bit-flip error probability is the sum of all the 56 Pauli errors involving a bit flip ( $X$ - or  $Y$ -error) and simulated in figure 9a. We found an exponential suppression of bit flips proportional to  $\exp^{-a|\alpha|^2}$  with  $a = 2.131 \pm 0.005$ . The reduced model provides also the phase flips ( $Z$ -error) in figure 9b. An illustration of  $64 \times 64$   $\chi^E$  matrix for the reduced propagator error  $E_{\text{red}}$  is given in appendix E, figure 15. A first-order computation of the leakage is shown in figure 17b.

## V. CONCLUDING REMARKS

We have introduced a new numerical method for simulating open quantum systems composed of several subsystems, exponentially stabilized towards stationary subspaces. This numerical method is based on a perturbation analysis with an original asymptotic expansion exploiting the reduced model formulation of the dynamics, relying on the invariant operators of the local and nominal dissipative dynamics of the subsystems. The derivation was shown up to a second-order expansion which can be computed with only local calculations for each subsystem. We have applied this method on several cat-qubit gates ( $Z$ ,  $ZZ$ ,  $ZZZ$ ,  $CNOT$  and  $CCNOT$ ) and shown that the dominant phase-flip error rates and the exponentially small bit-flip error rates are well described by such reduced-order models and simulations up to 16 photons in each cat-qubit.

The two-photon dissipation of the cat-qubit encoding comes from a more complex master equation involving a buffer mode coupled to the memory cavity via a two-photon exchange Hamiltonian, [34]. Similar analysis can thus be built with such composite cavity-buffer description for each cat-qubit.

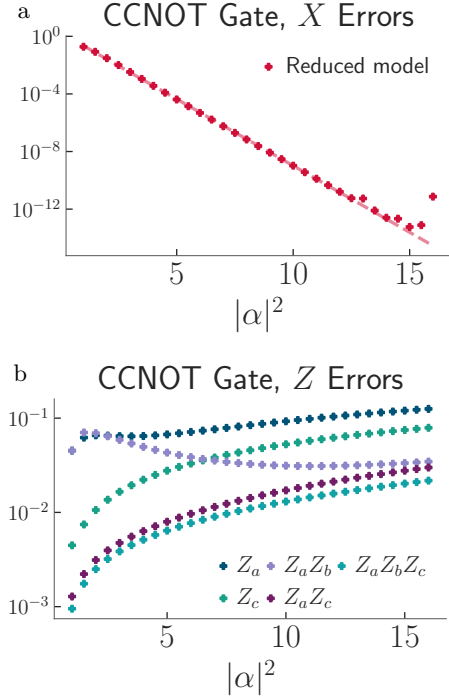


FIG. 9: Comparison between (a)  $X$  and (b)  $Z$  error probabilities of a CCNOT gate,  $p_{Z_a} = p_{Z_b}$  in dark blue,  $p_{Z_c}$  in green,  $p_{Z_a Z_b}$  in lavender,  $p_{Z_a Z_c} = p_{Z_b Z_c}$  in violet and  $p_{Z_a Z_b Z_c}$  in light blue, obtained via reduced model simulations (49) (colored plus) for different mean photon numbers  $|\alpha|^2$ . A simple fit yields an exponential suppression of bit-flips with an exponential coefficient of  $2.131 \pm 0.005$  (dashed line).

The derivations shown here can be further applied to other similar composite systems with dominant local stabilization used in autonomous quantum error correction schemes, such as squeezed cat-qubits [39, 40] or grid-states [41, 42].

This numerical method exploiting strong local dissipation with weak coupling and decoherence in many-body systems could also be useful, after some adaptation, in the development quantum circuit implementing quantum error correction as repetition code [43] or surface code [44].

## VI. ACKNOWLEDGMENTS

We thank Philippe Campagne-Ibarcq, Jérémie Guillaud, Mazhar Mirrahimi, Claude Le Bris, Alain Sarlette, Lev-Arcady Sellem and Antoine Tilloy for numerous discussions and scientific exchanges on model reduction, numerical simulations, cat-qubits and bosonic codes.

This project has received funding from the Plan France 2030 through the project ANR-22-PETQ-0006.

This project has received funding from the European Research Council (ERC) under the European Union's

Horizon 2020 research and innovation program (grant agreement No. [884762]).

The numerical simulations were performed using the

computer cluster of Inria Paris. The simulations in the full model picture were performed using the QuTiP open-source package.

- 
- [1] A. Wallraff et al. Approaching unit visibility for control of a superconducting qubit with dispersive readout. *Phys. Rev. Lett.*, 95:060501, Aug 2005.
  - [2] A. Blais et al. Circuit quantum electrodynamics. *Rev. Mod. Phys.*, 93:025005, May 2021.
  - [3] P. W. Shor. Scheme for reducing decoherence in quantum computer memory. *Phys. Rev. A*, 52(4):R2493–R2496, October 1995.
  - [4] D. G. Cory et al. Experimental quantum error correction. *Phys. Rev. Lett.*, 81:2152–2155, Sep 1998.
  - [5] J. Kempe et al. Theory of decoherence-free fault-tolerant universal quantum computation. *Phys. Rev. A*, 63:042307, Mar 2001.
  - [6] Dave Bacon. Operator quantum error-correcting subsystems for self-correcting quantum memories. *Phys. Rev. A*, 73:012340, Jan 2006.
  - [7] M. McEwen et al. Removing leakage-induced correlated errors in superconducting quantum error correction. *Nature Communications*, 12(1), Mar 2021.
  - [8] Z. Chen et al. Exponential suppression of bit or phase errors with cyclic error correction. *Nature*, 595(7867):383–387, 2021.
  - [9] S. Krinner et al. Realizing repeated quantum error correction in a distance-three surface code. *Nature*, 605(7911):669–674, 2022.
  - [10] A. Joshi, K. Noh, and Y. Gao. Quantum information processing with bosonic qubits in circuit QED. *Quantum Science and Technology*, 6(3):033001, April 2021.
  - [11] W. Cai et al. Bosonic quantum error correction codes in superconducting quantum circuits. *Fundamental Research*, 1(1):50–67, 2021.
  - [12] D. Gottesman, A. Kitaev, and J. Preskill. Encoding a qubit in an oscillator. *Physical Review A*, 64(1):012310, 2001.
  - [13] L. Hu et al. Quantum error correction and universal gate set operation on a binomial bosonic logical qubit. *Nature Physics*, 15(5):503–508, 2019.
  - [14] J. M. Gertler et al. Protecting a bosonic qubit with autonomous quantum error correction. *Nature*, 590(7845):243–248, 2021.
  - [15] N. Ofek et al. Extending the lifetime of a quantum bit with error correction in superconducting circuits. *Nature*, 536(7617):441–445, August 2016.
  - [16] V. V. Sivak et al. Real-time quantum error correction beyond break-even. *Nature*, 616(7955):50–55, mar 2023.
  - [17] L.-A. Sellem et al. A GKP qubit protected by dissipation in a high-impedance superconducting circuit driven by a microwave frequency comb. , <http://arxiv.org/abs/2304.01425>
  - [18] J. Guillaud and M. Mirrahimi. Repetition cat qubits for fault-tolerant quantum computation. *Phys. Rev. X*, 9:041053, Dec 2019.
  - [19] C. Chamberland et al. Building a fault-tolerant quantum computer using concatenated cat codes. *PRX Quantum*, 3:010329, Feb 2022.
  - [20] G. Pantaleoni, B. Q. Baragiola and N. C. Menicucci. Zak transform as a framework for quantum computation with the gottesman-kitaev-preskill code. *Physical Review A*, 107(6), jun 2023.
  - [21] D. S. Schlegel, F. Minganti, and V. Savona. Coherent-state ladder time-dependent variational principle for open quantum systems. <http://arxiv.org/abs/2306.13708>
  - [22] F. Verhulst. *Methods and Applications of Singular Perturbations: Boundary Layers and Multiple Timescale Dynamics*. Springer, 2005.
  - [23] P.V. Kokotovic and H.K. Kahlil. *Singular Perturbations in Systems and Control*. IEEE Press, New York, 1986.
  - [24] N. Fenichel. Geometric singular perturbation theory for ordinary differential equations. *J. Diff. Equations*, 31:53–98, 1979.
  - [25] E. Brion, L. H. Pedersen, and K. Mølmer. Adiabatic elimination in a lambda system. *Journal of Physics A: Mathematical and Theoretical*, 40(5):1033, 2007.
  - [26] P. Zanardi and L. Campos Venuti. Coherent quantum dynamics in steady-state manifolds of strongly dissipative systems. *Phys. Rev. Lett.*, 113(24):240406–, December 2014.
  - [27] R. Azouit, A. Sarlette, and P. Rouchon. Convergence and adiabatic elimination for a driven dissipative quantum harmonic oscillator. In *2015 54th IEEE Conference on Decision and Control (CDC)*, pages 6447–6453, Dec 2015.
  - [28] R. Azouit, F. Chittaro, A. Sarlette, and P. Rouchon. Towards generic adiabatic elimination for bipartite open quantum systems. *Quantum Science and Technology*, 2:044011, 2017.
  - [29] D. Burgarth et al. Generalized adiabatic theorem and strong-coupling limits. *Quantum*, 3:152, jun 2019.
  - [30] M. Tokieda et al. Complete positivity violation in higher-order quantum adiabatic. In *proceedings 2023 IFAC World Congress*, pp: 1408–1413 , <https://arxiv.org/abs/2211.11008>
  - [31] F.-M. Le Régent and P. Rouchon. Heisenberg formulation of adiabatic elimination for open quantum systems with two time-scales To appear in *Proceedings of IEEE 62st Conference on Decision and Control (CDC 2023)* <https://arxiv.org/abs/2303.17308>
  - [32] V. Albert and L. Jiang. Symmetries and conserved quantities in Lindblad master equations. *Phys. Rev. A*, 89(2):022118–, February 2014.
  - [33] T. Kato. *Perturbation Theory for Linear Operators*. Springer, 1966.
  - [34] M. Mirrahimi et al. Dynamically protected cat-qubits: a new paradigm for universal quantum computation. *New Journal of Physics*, 16:045014, 2014.
  - [35] Z. Leghtas et al. Confining the state of light to a quantum manifold by engineered two-photon loss. *Science*, 347(6224):853–857, February 2015.
  - [36] R. Azouit, A. Sarlette, and P. Rouchon. Well-posedness and convergence of the Lindblad master equation for a quantum harmonic oscillator with multi-photon drive



- and damping. *ESAIM: COCV*, 22(4):1353–1369, 2016.
- [37] S. Touzard et al. Coherent oscillations inside a quantum manifold stabilized by dissipation. *Phys. Rev. X*, 8:021005, Apr 2018.
  - [38] R. Lescanne et al. Exponential suppression of bit-flips in a qubit encoded in an oscillator. *Nat. Phys.*, 16:509–513, 2020.
  - [39] D. S. Schlegel, F. Minganti, and V. Savona. Quantum error correction using squeezed schrödinger cat states. *Physical Review A*, 106(2), 2022. Number: 2 Publisher: American Physical Society (APS).
  - [40] Qian Xu et al. Autonomous quantum error correction and fault-tolerant quantum computation with squeezed cat qubits, 2022. <https://arxiv.org/abs/2210.13406>.
  - [41] B. Royer, S. Singh, and S. Girvin. Stabilization of finite-energy Gottesman-Kitaev-Preskill states. *Phys. Rev. Lett.*, 125:260509, Dec 2020.
  - [42] L.-A. Sellem et al. Exponential convergence of a dissipative quantum system towards finite-energy grid states of an oscillator. *Proceedings of IEEE 61st Conference on Decision and Control (CDC 2022)*, pages 5149–5154, 2022.
  - [43] J. Guillaud and M. Mirrahimi. Error rates and resource overheads of repetition cat qubits. *Phys. Rev. A*, 103(4), 2021..
  - [44] A. Fowler et al. Surface codes: Towards practical large-scale quantum computation. *Phys. Rev. A*, 86(3):032324, 2012.
  - [45] A. N. Jordan et al. Anatomy of fluorescence: quantum trajectory statistics from continuously measuring spontaneous emission. *Quantum Studies: Mathematics and Foundations*, 3(3):237–263, 2016.

## Appendix A: High-order expansion and simulations

### 1. Expansion order exceeding 2

Take  $n \geq 2$  and assume that we have computed all the terms  $F_{d',d}^{(r)}$  and  $\hat{S}_{d'}^{(r)}$  of order  $r < n$  with  $\text{Tr}(\hat{J}_{d'} \hat{S}_d^{(r)}) = 0$  for all  $d$  and  $d'$ . Invariance condition of order  $n$  reads

$$\forall d \in \{1, \dots, \bar{d}\},$$

$$\sum_{d''=1}^{\bar{d}} \sum_{r=1}^n F_{d'',d}^{(r)} \hat{S}_{d''}^{(n-r)} = \mathcal{L}_0(\hat{S}_d^{(n)}) + \mathcal{L}_1(\hat{S}_d^{(n-1)}).$$

Left multiplication by operator  $\hat{J}_{d'}$  and taking the trace yields

$$F_{d',d}^{(n)} = \text{Tr}(\hat{J}_{d'} \mathcal{L}_1(\hat{S}_d^{(n-1)})) = \text{Tr}(\mathcal{L}_1^*(\hat{J}_{d'}) \hat{S}_d^{(n-1)}). \quad (\text{A1})$$

For  $\hat{S}_d^{(n)}$  we take the solution of

$$\mathcal{L}_0(\hat{X}) = \sum_{d''=1}^{\bar{d}} \sum_{r=1}^n F_{d'',d}^{(r)} \hat{S}_{d''}^{(n-r)} - \mathcal{L}_1(\hat{S}_d^{(n-1)})$$

such that, for all  $d'$ ,  $\text{Tr}(\hat{J}_{d'} \hat{X}) = 0$ :

$$\hat{S}_d^{(n)} = \bar{\mathcal{R}}_0 \left( \mathcal{L}_1(\hat{S}_d^{(n-1)}) - \sum_{d''=1}^{\bar{d}} \sum_{r=1}^n F_{d'',d}^{(r)} \hat{S}_{d''}^{(n-r)} \right)$$

$$= \int_0^{+\infty} e^{s\mathcal{L}_0} \left( \mathcal{L}_1(\hat{S}_d^{(n-1)}) - \sum_{d''=1}^{\bar{d}} \sum_{r=1}^n F_{d'',d}^{(r)} \hat{S}_{d''}^{(n-r)} \right) ds. \quad (\text{A2})$$

Since  $\bar{\mathcal{K}}_0(\hat{S}_{d''}^{n-r}) = 0$  for any  $r \in \{1, n-1\}$  and  $\bar{\mathcal{K}}_0(\mathcal{L}_1(\hat{S}_d^{(n-1)})) = \sum_{d''=1}^{\bar{d}} F_{d'',d}^{(n)} \hat{S}_{d''}^{(0)}$ , the above integral is absolutely convergent.

With such asymptotic expansion, we get an order  $n$  approximation of the dynamics on the invariant slow-manifold  $\mathcal{D}_\epsilon$ , a reduced dynamical model of (1) based on the following  $\bar{d}$  dimensional linear system:

$$\frac{d}{dt} x(t) = \left( \sum_{r=1}^n \epsilon^r F^{(r)} \right) x(t) \quad (\text{A3})$$

where  $\rho_t = \sum_{d=1}^{\bar{d}} x_d(t) \left( \sum_{r=0}^n \epsilon^r \hat{S}_d^{(r)} \right)$  satisfies (1) up to  $\epsilon^{n+1}$  terms. Here  $F^{(r)}$  is the matrix of real entries  $F_{d,d'}^{(r)}$ . Since  $x_d = \text{Tr}(\hat{J}_d \rho_t)$ , the dynamical system (A3) is an approximation of order  $n$  for the reduced model slow dynamics of the nominal invariant operators  $\hat{J}_d$ : Up-to  $\epsilon^{n+1}$  corrections we have in the reduced model picture:

$$\forall d \in \{1, \dots, \bar{d}\},$$

$$\frac{d}{dt} \hat{J}_d \triangleq \mathcal{L}_0^*(\hat{J}_d) + \epsilon \mathcal{L}_1^*(\hat{J}_d) = \sum_{d'=1}^{\bar{d}} \sum_{r=1}^n \epsilon^r F_{d,d'}^{(r)} \hat{J}_{d'} + O(\epsilon^{n+1}).$$

## 2. Z-gate simulations up to order 5

An example of such higher order approximation using Eqs. A2 and A3 is given in figure 10 and figure 11 for the case of a cat-qubit on which we perform a Z gate as in Sec. II B with  $|\alpha|^2 = 4$ . For the error probabilities, we see that the second-order expansion is already very accurate, and the third-order expansion is almost indistinguishable from higher order expansions. Regarding leakage, we see that first-order leakage is not enough to capture the leakage dynamics, but that second-order leakage is already very accurate and indistinguishable from higher order expansions figure 11.

## Appendix B: Second-order approximation with slow time dependency

Here we only derive the second-order approximation with slow time dependency. We are looking for solutions of the perturbed system

$$\frac{d}{dt} \rho_t = \mathcal{L}_0(\rho_t) + \epsilon \mathcal{L}_1(\epsilon t, \rho_t) \quad (\text{B1})$$

based on the following asymptotic expansion:  $\rho_t = \sum_{d=1}^{\bar{d}_0} x_{d,t} \left( \hat{S}_d^{(0)} + \hat{S}_d^{(1)} \right)$  where

$$X_{t+1} = \left( F^{(0)} + F^{(1)} + F^{(2)} \right) X_t$$

with  $F^{(0)} = I$ ,  $X_t = (x_{1,t}, \dots, x_{\bar{d}_0,t})^T$ . We assume that the GKSL superoperator  $\mathcal{L}_1$  in (1) depends slowly on time, i.e., that the operators  $\hat{H}_1$  and  $\hat{L}_{1,\nu}$  are smooth functions of  $\epsilon t$ :

$$\mathcal{L}_1(\epsilon t, \rho) = -i[\hat{H}_1(\epsilon t), \rho] + \sum_{\nu} \hat{L}_{1,\nu}(\epsilon t) \rho \hat{L}_{1,\nu}^\dagger(\epsilon t)$$

$$- \frac{1}{2} \left( \hat{L}_{1,\nu}^\dagger(\epsilon t) \hat{L}_{1,\nu}(\epsilon t) \rho + \rho \hat{L}_{1,\nu}^\dagger(\epsilon t) \hat{L}_{1,\nu}(\epsilon t) \right).$$

Then for each  $n$ ,  $F_{d',d}^{(n)}$  and  $\hat{S}_d^{(n)}$  depend also on  $\epsilon t$ . Thus, the invariance condition (6) becomes

$$\sum_{d=1}^{\bar{d}} \left( \frac{dx_d}{dt} \hat{S}_d(\epsilon) + x_d \frac{d}{dt} \hat{S}_d(\epsilon) \right) = (\mathcal{L}_0 + \epsilon \mathcal{L}_1) \left( \sum_{d=1}^{\bar{d}} x_d \hat{S}_d(\epsilon) \right)$$

where  $F_{d,d'}(\epsilon t, \epsilon) = \sum_{n \geq 0} \epsilon^n F_{d,d'}^{(n)}(\epsilon t)$  and  $\hat{S}_d(\epsilon t, \epsilon) = \sum_{n \geq 0} \epsilon^n \hat{S}_d^{(n)}(\epsilon t)$ . One has to identify terms with same orders versus  $\epsilon$  in

$$\forall d \in \{1, \dots, \bar{d}\},$$

$$\sum_{n \geq 0} \epsilon^n \frac{d}{dt} \hat{S}_d^{(n)} + \sum_{d'=1}^{\bar{d}} \left( \sum_{n \geq 0} \epsilon^n F_{d',d}^{(n)} \right) \left( \sum_{n' \geq 0} \epsilon^{n'} \hat{S}_{d'}^{(n')} \right)$$

$$= (\mathcal{L}_0 + \epsilon \mathcal{L}_1) \left( \sum_{n \geq 0} \epsilon^n \hat{S}_d^{(n)} \right), \quad (\text{B2})$$

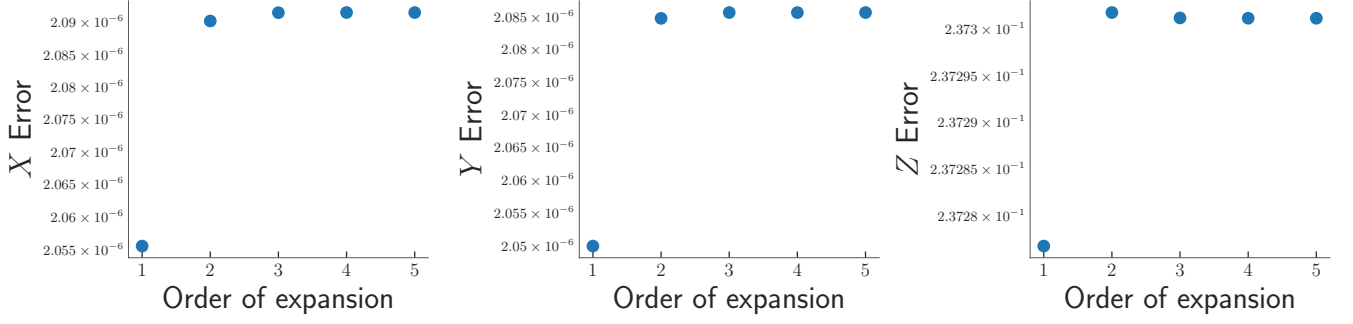


FIG. 10: Convergence of the  $X$ ,  $Y$  and  $Z$  error probabilities by increasing the order of the perturbative analysis from 1 to 5. The error probabilities are computed for a cat qubit on which we perform a  $Z$  gate as in Sec. II B with  $|\alpha|^2 = 4$ . The second-order expansion is already very accurate, and the third-order expansion is almost indistinguishable from higher order expansions.

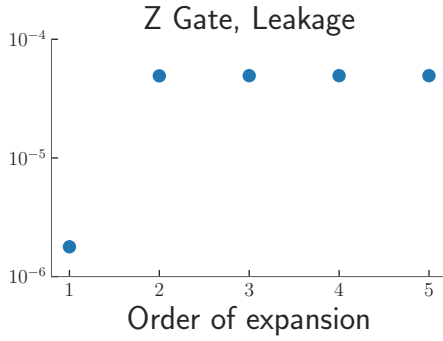


FIG. 11: Up to 5<sup>th</sup>-order leakage of the  $Z$  gate starting from the  $|\mathcal{C}_\alpha^+\rangle$  and ending in  $|\mathcal{C}_\alpha^-\rangle$  for a cat-qubit with  $|\alpha|^2 = 4$  and the same simulation parameters as in Sec. II B. All orders  $\geq 2$  are superposed.

using the fact that, for each  $n$ ,  $\frac{d}{dt}\hat{S}^{(n)}(\epsilon t)$  is of order  $\epsilon$ .

The zero-order condition is satisfied with  $F_{d,d'}^{(0)} = 0$  and  $\hat{S}_d^{(0)} = \hat{S}_d$ . First-order condition remains unchanged and yields as in (13) and (16) to

$$F_{d',d}^{(1)}(\epsilon t) = \text{Tr} \left( \hat{J}_{d'} \mathcal{L}_1(\epsilon t, \hat{S}_d) \right)$$

with

$$\hat{S}_d^{(1)}(\epsilon t) = \int_0^{+\infty} e^{s\mathcal{L}_0} \left( \mathcal{L}_1(\epsilon t, \hat{S}_d) - \bar{\mathcal{K}}_0(\mathcal{L}_1(\epsilon t, \hat{S}_d)) \right) ds \quad (\text{B3})$$

where  $\text{Tr} \left( \hat{J}_{d'} \hat{S}_d^{(1)}(\epsilon t) \right) = 0$  and thus  $\text{Tr} \left( \hat{J}_{d'} \frac{d}{dt} \hat{S}_d^{(1)}(\epsilon t) \right) = 0$ , for all  $d'$  and  $t$ . The second-

order condition is:

$$\begin{aligned} \forall d \in \{1, \dots, \bar{d}\}, \\ \frac{d}{d(\epsilon t)} \hat{S}_d^{(1)}(\epsilon t) + \sum_{d''=1}^{\bar{d}} \left( F_{d'',d}^{(1)}(\epsilon t) \hat{S}_{d''}^{(1)}(\epsilon t) + F_{d'',d}^{(2)} \hat{S}_{d''} \right) \\ = \mathcal{L}_0(\hat{S}_d^{(2)}) + \mathcal{L}_1(\epsilon t, \hat{S}_d^{(1)}(\epsilon t)). \quad (\text{B4}) \end{aligned}$$

Multiplying by  $\hat{J}_{d'}$  and taking the trace show that the second-order correction formula is identical to the one for time-invariant  $\mathcal{L}_1$ . To summarize, we have either for time-invariant or slowly time-varying  $\mathcal{L}_1$ , the following second-order approximation formula for the dynamics of  $x$ :

$$\forall d' \in \{1, \dots, \bar{d}\}, \quad \frac{d}{dt} x_{d'} = \sum_{d=1}^{\bar{d}} \left( \epsilon F_{d',d}^{(1)}(\epsilon t) + \epsilon^2 F_{d',d}^{(2)}(\epsilon t) \right) x_d \quad (\text{B5})$$

with

$$\begin{aligned} F_{d',d}^{(1)}(\epsilon t) &= \text{Tr} \left( \hat{J}_{d'} \mathcal{L}_1(\epsilon t, \hat{S}_d) \right), \\ F_{d',d}^{(2)}(\epsilon t) &= \text{Tr} \left( \mathcal{L}_1^*(\epsilon t, \hat{J}_{d'}) \bar{\mathcal{R}}_0 \left( \mathcal{L}_1(\epsilon t, \hat{S}_d) \right) \right) \quad (\text{B6}) \end{aligned}$$

where  $\bar{\mathcal{R}}_0$  is defined in (17).

### Appendix C: Time discretization of continuous-time quantum master equation

We propose here an adapted numerical scheme to convert the continuous-time dynamics (1) into a discrete-time dynamic (D1).

Take a time-step  $\delta t > 0$  very small compared to evolution time-constant of (1). An exact quantum channel approximation of  $e^{\delta t \mathcal{L}_0}$  identical, up to  $\delta t^2$  terms to the explicit Euler scheme, is the following (see [45, appendix

B]):

$$\begin{aligned} \rho_{t+\delta t} &= \mathcal{K}_0(\rho_t) \\ &\left( = e^{\delta t \mathcal{L}_0}(\rho_t) + O(\delta t^2) = \rho_t + \delta t \mathcal{L}_0(\rho_t) + O(\delta t^2) \right) \end{aligned} \quad (\text{C1})$$

where  $\mathcal{K}_0$  admits the following Kraus structure:

$$\begin{aligned} \mathcal{K}_0(\rho) &= \widehat{U}_0 \left( \widehat{\mathbf{M}}_0 \widehat{U}_0 \rho \widehat{U}_0^\dagger \widehat{\mathbf{M}}_0^\dagger \right. \\ &\quad \left. + \delta t \left( \sum_\nu \widehat{\mathbf{L}}_{0,\nu} \widehat{U}_0 \rho \widehat{U}_0^\dagger \widehat{\mathbf{L}}_{0,\nu}^\dagger \right) \right) \widehat{U}_0^\dagger \end{aligned} \quad (\text{C2})$$

with

$$\widehat{U}_0 = e^{-i\delta t \widehat{H}_0/2}, \quad \widehat{\mathbf{M}}_0 = \widehat{M}_0 \widehat{W}_0^{-1/2}, \quad \widehat{\mathbf{L}}_{0,\nu} = \widehat{L}_{0,\nu} \widehat{W}_0^{-1/2} \quad (\text{C3})$$

where

$$\begin{aligned} \widehat{M}_0 &= I - \sum_\nu \frac{\delta t}{2} \widehat{L}_{0,\nu}^\dagger \widehat{L}_{0,\nu}, \\ \widehat{W}_0 &= \widehat{M}_0^\dagger \widehat{M}_0 + \delta t \sum_\nu \widehat{L}_{0,\nu}^\dagger \widehat{L}_{0,\nu}. \end{aligned}$$

Take as perturbation  $\mathcal{K}_1$  the simplest approximation:

$$\mathcal{K}_1(\rho) = \delta t \mathcal{L}_1(\rho). \quad (\text{C4})$$

## Appendix D: Adiabatic elimination in discrete-time

### 1. Single system

When  $t$  is an integer, (1) is replaced by

$$\rho_{t+1} = \mathcal{K}_0(\rho_t) + \epsilon \mathcal{K}_1(\rho_t) \quad (\text{D1})$$

where  $\mathcal{K}_0$  is a quantum channel stabilizing the subspace  $\mathcal{D}_0$  spanned by the orthonormal basis  $\widehat{S}_d$  and with invariant operator  $\widehat{J}_d = \lim_{t \rightarrow +\infty} (\mathcal{K}_0^*)^t(\widehat{S}_d)$  where  $(\mathcal{K}_0^*)^t$  corresponds to  $t$  iterates of the adjoint map  $\mathcal{K}_0^*$ . For any  $\rho_0$  we have

$$\lim_{t \rightarrow +\infty} (\mathcal{K}_0^*)^t(\rho_0) = \overline{\mathcal{K}}_0(\rho_0) = \sum_d \text{Tr} \left( \widehat{J}_d \rho_0 \right) \widehat{S}_d. \quad (\text{D2})$$

Invariance condition (6) reads then

$$\sum_{d=1}^{\bar{d}} x_d(t+1) \widehat{S}_d(\epsilon) = (\mathcal{K}_0 + \epsilon \mathcal{K}_1) \left( \sum_{d=1}^{\bar{d}} x_d(t) \widehat{S}_d(\epsilon) \right) \quad (\text{D3})$$

with  $x_d(t+1) = \sum_{d'} F_{d,d'}(\epsilon) x_{d'}(t)$ . Combined with the series expansion of  $\widehat{S}_d(\epsilon)$  and  $F_{d,d'}(\epsilon)$  it yields:

$$\begin{aligned} \forall d \in \{1, \dots, \bar{d}\}, \\ \sum_{d'=1}^{\bar{d}} \left( \sum_{n \geq 0} \epsilon^n F_{d',d}^{(n)} \right) \left( \sum_{n' \geq 0} \epsilon^{n'} \widehat{S}_{d'}^{(n')} \right) \\ = (\mathcal{K}_0 + \epsilon \mathcal{K}_1) \left( \sum_{n \geq 0} \epsilon^n \widehat{S}_d^{(n)} \right). \end{aligned}$$

The zero-order term is satisfied with  $F_{d,d'}^{(0)} = \delta_{d,d'}$  and  $\widehat{S}_d^{(0)} = \widehat{S}_d$ . First-order conditions read

$$\begin{aligned} \forall d \in \{1, \dots, \bar{d}\}, \\ \widehat{S}_d^{(1)} + \sum_{d''=1}^{\bar{d}} F_{d'',d}^{(1)} \widehat{S}_{d''}^{(0)} = \mathcal{K}_0(\widehat{S}_d^{(1)}) + \mathcal{K}_1(\widehat{S}_d^{(0)}). \end{aligned}$$

Left multiplication by operator  $\widehat{J}_{d'}$  and taking the trace yields

$$F_{d',d}^{(1)} = \text{Tr} \left( \widehat{J}_{d'} \mathcal{K}_1(\widehat{S}_d) \right) \quad (\text{D4})$$

since  $\text{Tr} \left( \widehat{J}_{d'} \widehat{S}_{d''}^{(0)} \right) = \delta_{d',d''}$  and  $\text{Tr} \left( \widehat{J}_{d'} \mathcal{K}_0(\widehat{W}) \right) = \text{Tr} \left( \widehat{J}_{d'} \widehat{W} \right)$  for any operator  $\widehat{W}$  because  $\mathcal{K}_0^*(\widehat{J}_{d'}) = \widehat{J}_{d'}$ . Thus,  $\widehat{S}_d^{(1)}$  is a solution  $\widehat{X}$  of the following equation:

$$\widehat{X} = \mathcal{K}_0(\widehat{X}) + \mathcal{K}_1(\widehat{S}_d^{(0)}) - \sum_{d''=1}^{\bar{d}} F_{d'',d}^{(1)} \widehat{S}_{d''}^{(0)}$$

Since the quantum channel  $\mathcal{K}_0$  is a contraction with a rate assumed to be strictly less than 1, the following solution is chosen,

$$\widehat{S}_d^{(1)} = \sum_{s \geq 0} (\mathcal{K}_0)^s \left( \mathcal{K}_1(\widehat{S}_d^{(0)}) - \overline{\mathcal{K}}_0(\mathcal{K}_1(\widehat{S}_d^{(0)})) \right),$$

based on this absolutely converging series and satisfying  $\text{Tr} \left( \widehat{J}_{d'} \widehat{S}_d^{(1)} \right) = 0$  for all  $d'$ . This defines the superoperator

$$\overline{\mathcal{R}}_0(\widehat{W}) = \sum_{s=0}^{+\infty} (\mathcal{K}_0)^s (\widehat{W} - \overline{\mathcal{K}}_0(\widehat{W}))$$

where  $(\mathcal{K}_0)^0$  stands for identity.

Take  $n \geq 2$  and assume that we have computed all the terms  $F_{d',d}^{(r)}$  and  $\widehat{S}_{d'}^{(r)}$  of order  $r < n$  with  $\text{Tr} \left( \widehat{J}_{d'} \widehat{S}_d^{(r)} \right) = 0$  for all  $d$  and  $d'$ . Invariance condition of order  $n$  reads

$$\begin{aligned} \forall d \in \{1, \dots, \bar{d}\}, \\ \widehat{S}_d^{(n)} + \sum_{d''=1}^{\bar{d}} \sum_{r=1}^n F_{d'',d}^{(r)} \widehat{S}_{d''}^{(n-r)} = \mathcal{K}_0(\widehat{S}_d^{(n)}) + \mathcal{K}_1(\widehat{S}_d^{(n-1)}). \end{aligned}$$

Left multiplication by operator  $\hat{J}_{d'}$  and taking the trace yields

$$F_{d',d}^{(n)} = \text{Tr} \left( \hat{J}_{d'} \mathcal{K}_1(\hat{S}_d^{(n-1)}) \right) = \text{Tr} \left( \mathcal{K}_1^*(\hat{J}_{d'}) \hat{S}_d^{(n-1)} \right).$$

For  $\hat{S}_d^{(n)}$  we take the solution such that, for all  $d'$ ,  $\text{Tr} \left( \hat{J}_{d'} \hat{S}_d^{(n)} \right) = 0$ :

$$\begin{aligned} \hat{S}_d^{(n)} &= \bar{\mathcal{R}}_0 \left( \mathcal{K}_1(\hat{S}_d^{(n-1)}) - \sum_{d''=1}^{\bar{d}} \sum_{r=1}^n F_{d'',d}^{(r)} \hat{S}_{d''}^{(n-r)} \right) \dots \\ &\dots = \sum_{s \geq 0} (\mathcal{K}_0)^s \left( \mathcal{K}_1(\hat{S}_d^{(n-1)}) - \sum_{d''=1}^{\bar{d}} \sum_{r=1}^n F_{d'',d}^{(r)} \hat{S}_{d''}^{(n-r)} \right). \end{aligned}$$

The discrete-time reduced model is then

$$x(t+1) = x(t) + \left( \sum_{r=1}^n \epsilon^r F^{(r)} \right) x(t) \quad (\text{D5})$$

with  $\rho_t = \sum_{d=1}^{\bar{d}} x_d(t) \left( \sum_{r=0}^n \epsilon^r \hat{S}_d^{(r)} \right)$  satisfying (D1) up to  $\epsilon^{n+1}$  correction and for any  $d$ ,  $x_d(t) = \text{Tr} \left( \hat{J}_d \rho_t \right)$ . Up to  $\epsilon^{n+1}$  corrections, we have the following reduced model dynamics for the invariant operators

$$\begin{aligned} \forall d \in \{1, \dots, \bar{d}\}, \\ \hat{J}_d(t+1) &\triangleq \mathcal{K}_0^*(\hat{J}_d(t)) + \epsilon \mathcal{K}_1^*(\hat{J}_d(t)) \\ &= \hat{J}_d(t) + \sum_{d'=1}^{\bar{d}} \sum_{r=1}^n \epsilon^r F_{d,d'}^{(r)} \hat{J}_{d'}(t) + O(\epsilon^{n+1}). \end{aligned}$$

The discrete-time version of equation (20) providing the second-order approximation reads

$$\begin{aligned} F_{d',d}^{(1)} &= \text{Tr} \left( \hat{J}_{d'} \mathcal{K}_1(\hat{S}_d) \right), \\ F_{d',d}^{(2)} &= \text{Tr} \left( \mathcal{K}_1^*(\hat{J}_{d'}) \bar{\mathcal{R}}_0 \left( \mathcal{K}_1(\hat{S}_d) \right) \right) \quad (\text{D6}) \end{aligned}$$

and remains valid for slowly time-varying perturbation, i.e., for  $\mathcal{K}_1(\epsilon t, \rho)$  where the dependence versus  $\epsilon t$  of  $\mathcal{K}_1$  is smooth:

$$\begin{aligned} F_{d',d}^{(1)}(\epsilon t) &= \text{Tr} \left( \hat{J}_{d'} \mathcal{K}_1(\epsilon t, \hat{S}_d) \right), \\ F_{d',d}^{(2)}(\epsilon t) &= \text{Tr} \left( \mathcal{K}_1^*(\epsilon t, \hat{J}_{d'}) \bar{\mathcal{R}}_0 \left( \mathcal{K}_1(\epsilon t, \hat{S}_d) \right) \right) \quad (\text{D7}) \end{aligned}$$

## 2. Composite systems

Discrete-time bipartite structure is based on

$$\mathcal{K}_0 = \mathcal{K}_{A,0} \otimes \mathcal{K}_{B,0} \quad (\text{D8})$$

where  $\mathcal{K}_{A,0}$  and  $\mathcal{K}_{B,0}$  are local quantum maps on  $\mathcal{H}_A$  and  $\mathcal{H}_B$  stabilizing the local subspaces  $\mathcal{D}_{A,0}$  and  $\mathcal{D}_{B,0}$ .

Their dimensions are  $\bar{d}_A$  and  $\bar{d}_B$  with  $(\hat{S}_{A,d_A})_{1 \leq d_A \leq \bar{d}_A}$  and  $(\hat{S}_{B,d_B})_{1 \leq d_B \leq \bar{d}_B}$  as orthonormal basis of Hermitian operators. We assume that  $\mathcal{K}_{A,0}$  and  $\mathcal{K}_{B,0}$  ensure exponential convergence towards  $\mathcal{D}_{A,0}$  and  $\mathcal{D}_{B,0}$ : for any operators on  $\mathcal{H}$ ,

$$\lim_{t \rightarrow +\infty} (\mathcal{K}_{A,0})^t \otimes (\mathcal{K}_{B,0})^t (\rho_0) = \bar{\mathcal{K}}_0(\rho_0)$$

where  $\bar{\mathcal{K}}_0$  remains given by (34) with  $\hat{J}_{A,d_A}$  and  $\hat{J}_{B,d_B}$  as follows:

$$\begin{aligned} \hat{J}_{A,d_A} &= \lim_{t \rightarrow +\infty} (\mathcal{K}_{A,0}^*)^t (\hat{S}_{A,d_A}), \\ \hat{J}_{B,d_B} &= \lim_{t \rightarrow +\infty} (\mathcal{K}_{B,0}^*)^t (\hat{S}_{B,d_B}). \end{aligned}$$

Assume the super operator  $\mathcal{K}_1$  only involve finite sums of tensor products of operators on  $\mathcal{H}_A$  and  $\mathcal{H}_B$ . This means that for any  $\hat{X}_A$  and  $\hat{X}_B$  local operators on  $\mathcal{H}_A$  and  $\mathcal{H}_B$ ,

$$\mathcal{K}_1(\hat{X}_A \otimes \hat{X}_B) = \sum_{\nu=1}^{\bar{\nu}} \hat{L}_{A,\nu} \hat{X}_A \hat{R}_{A,\nu} \otimes \hat{L}_{B,\nu} \hat{X}_B \hat{R}_{B,\nu} \quad (\text{D9})$$

where  $\bar{\nu}$  is a positive integer, where  $\hat{L}_{A,\nu}$ ,  $\hat{R}_{A,\nu}$  are operators on  $\mathcal{H}_A$  and where  $\hat{L}_{B,\nu}$ ,  $\hat{R}_{B,\nu}$  are operators on  $\mathcal{H}_B$ .

The discrete-time analogue of (37) reads:

$$\begin{aligned} F_{(d'_A, d'_B), (d_A, d_B)}^{(1)} &= \sum_{\nu=1}^{\bar{\nu}} \text{Tr} \left( \hat{J}_{A,d'_A} \hat{S}_{A,d_A,\nu} \right) \text{Tr} \left( \hat{J}_{B,d'_B} \hat{S}_{B,d_B,\nu} \right) \\ &= \sum_{\nu=1}^{\bar{\nu}} \text{Tr} \left( \hat{S}_{A,d_A} \hat{J}_{A,d'_A,\nu} \right) \text{Tr} \left( \hat{S}_{B,d_B} \hat{J}_{B,d'_B,\nu} \right), \quad (\text{D10}) \end{aligned}$$

where for  $X = A, B$

$$\hat{J}_{X,d'_X,\nu} = \hat{R}_{X,\nu} \hat{J}_{X,d'_X} \hat{L}_{X,\nu}, \quad \hat{S}_{X,d_X,\nu} = \hat{L}_{X,\nu} \hat{S}_{X,d_X} \hat{R}_{X,\nu}. \quad (\text{D11})$$

Similarly, we derive from (44) the second-order discrete-time matrix  $F^{(2)}$ :

$$\begin{aligned} F_{(d'_A, d'_B), (d_A, d_B)}^{(2)} &= \sum_{\nu, \nu'=1}^{\bar{\nu}} \sum_{s=0}^{+\infty} \left( \text{Tr} \left( \hat{J}_{A,d'_A,\nu'} (\mathcal{K}_{A,0})^s (\hat{S}_{A,d_A,\nu}) \right) \right. \\ &\quad \times \text{Tr} \left( \hat{J}_{B,d'_B,\nu'} (\mathcal{K}_{B,0})^s (\hat{S}_{B,d_B,\nu}) \right) \dots \\ &\quad \left. \dots - G_{A,d'_A,d_A,\nu,\nu'} G_{B,d'_B,d_B,\nu,\nu'} \right), \quad (\text{D12}) \end{aligned}$$

where

$$G_{X,d'_X,d_X,\nu,\nu'} = \sum_{d''_X} \text{Tr} \left( \hat{J}_{X,d'_X} \hat{S}_{X,d''_X,\nu'} \right) \text{Tr} \left( \hat{J}_{X,d''_X} \hat{S}_{X,d_X,\nu} \right)$$

for  $X = A, B$ .

## Appendix E: Propagator simulation results

In this appendix, we give examples of  $\chi$  error-matrices defined in (46) for the ZZ-gate in figure 12, the ZZZ gate in figure 13, the CNOT gate in figure 14 and the Toffoli gate in figure 15 from which we extracted the Pauli error models shown in the main text, i.e., the diagonal of the  $\chi$  error-matrix used in quantum process tomography.

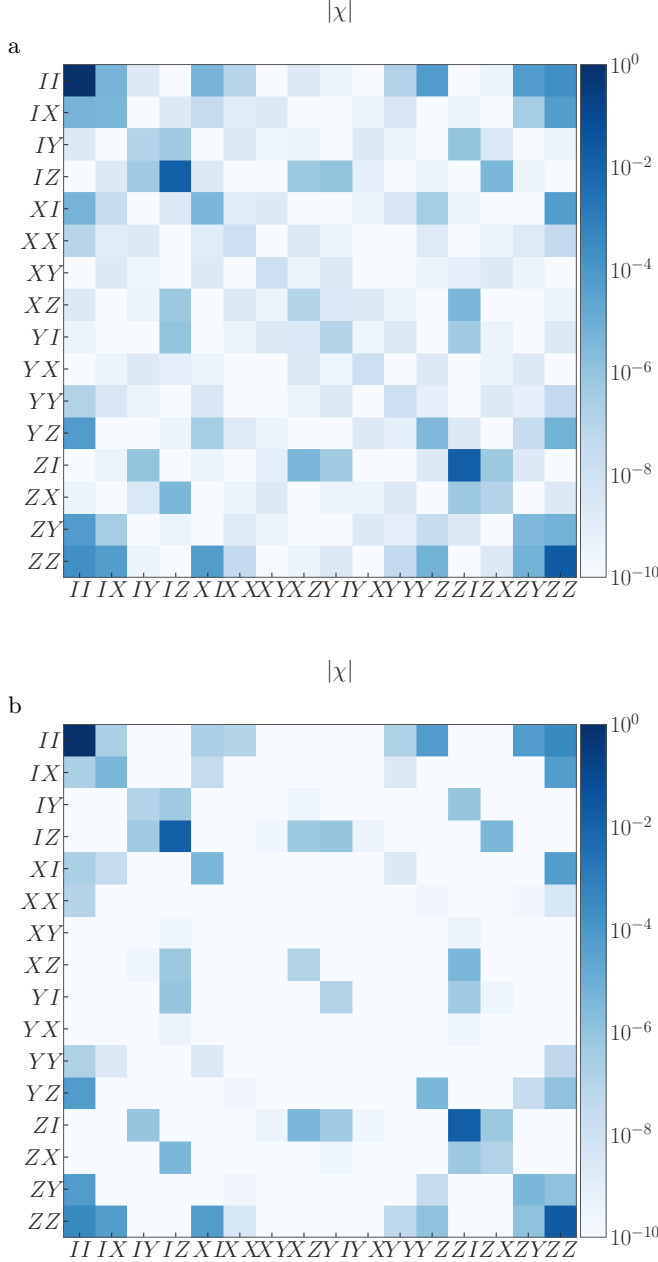


FIG. 12:  $\chi$  error-matrix of the ZZ gate with (a) full model, Galerkin truncation to 41 photons and (b) second-order reduced model where  $\alpha = 2, \kappa_1 = \frac{\kappa_2}{100}, \epsilon_Z = \frac{\kappa_2}{20}$ .

## Appendix F: Leakage computation

### 1. Single-mode leakage

The equation (16) allows to perform a first-order computation of the leakage, defined as the population outside the code space. If we define  $\hat{I}_c$  to be the projector on the code space of our system, then the population of the state  $\rho_t$  at a given time  $t$  inside the code space is  $\text{Tr}(\hat{I}_c \rho_t)$ . In the context of cat-qubit, the code space projector is defined by

$$\hat{I}_c = (|c_\alpha^+\rangle\langle c_\alpha^+| + |c_\alpha^-\rangle\langle c_\alpha^-|) \sim \sqrt{2}\hat{S}_1.$$

So for any state written at first-order  $\rho_t = \sum_{d=1}^{d_0} x_{d,t} (\hat{S}_d^{(0)} + \hat{S}_d^{(1)})$ , the leakage  $l$  is given by:

$$l(t) = 1 - \text{Tr}(\hat{I}_c \rho_t) = 1 - \sum_{d=1}^{d_0} x_{d,t} c_d \quad (\text{F1})$$

where

$$c_d = \text{Tr}(\hat{I}_c (\hat{S}_d^{(0)} + \hat{S}_d^{(1)})) = \sqrt{2}\delta_{1,d} + \text{Tr}(\hat{I}_c \bar{\mathcal{R}}_0(\mathcal{L}_1(\hat{S}_d))) \quad (\text{F2})$$

### 2. Composite-system leakage

In the case of a composite system, we can still compute the leakage at first-order, using the generalization of equation (16). For  $(d_A, d_B)$ , we define  $c_{d_A, d_B}$  as:  $c_{d_A, d_B} = \text{Tr}(\hat{I}_{c,A} \hat{I}_{c,B} \hat{S}_{d_A, d_B}(\epsilon))$  where  $\hat{S}_{d_A, d_B}(\epsilon) = \hat{S}_{d_A, d_B}^{(0)} + \hat{S}_{d_A, d_B}^{(1)}$  with  $\hat{S}_{d_A, d_B}^{(0)} = \hat{S}_{A, d_A}^{(0)} \hat{S}_{B, d_B}^{(0)}$  and

$$\hat{S}_{d_A, d_B}^{(1)} = \bar{\mathcal{R}}_0(\mathcal{L}_1(\hat{S}_{d_A, d_B}^{(0)})) = \sum_{\nu=1}^{\bar{\nu}} \bar{\mathcal{R}}_0(\hat{S}_{A, d_A, \nu} \otimes \hat{S}_{B, d_B, \nu}).$$

So we find that  $c_{d_A, d_B} = 2\delta_{1, d_A} \delta_{1, d_B} + \sum_{\nu=1}^{\bar{\nu}} \text{Tr}(\hat{I}_{c,A} \hat{I}_{c,B} \bar{\mathcal{R}}_0(\hat{S}_{A, d_A, \nu} \otimes \hat{S}_{B, d_B, \nu}))$ .

And finally, the leakage  $l$  of a state  $\rho_t = \sum_{d_A, d_B} x_{d_A, d_B, t} \hat{S}_{d_A, d_B}$  is given by:

$$l(t) = 1 - \text{Tr}(\hat{I}_c \rho_t) = 1 - \sum_{d_A, d_B=1}^{d_0} x_{d_A, d_B, t} c_{d_A, d_B} \quad (\text{F3})$$

However, second-order leakage can be obtained numerically via the following relation

$$\text{Tr}(\hat{I}_c \hat{S}_d^{(2)}) = \text{Tr}\left(\bar{\mathcal{R}}_0^*(\hat{I}_c) \left(\mathcal{L}_1(\hat{S}_d^{(1)}) - \sum_{d''=1}^{\bar{d}} F_{d'', d}^{(1)} \hat{S}_{d''}^{(1)}\right)\right)$$

with only local computations.



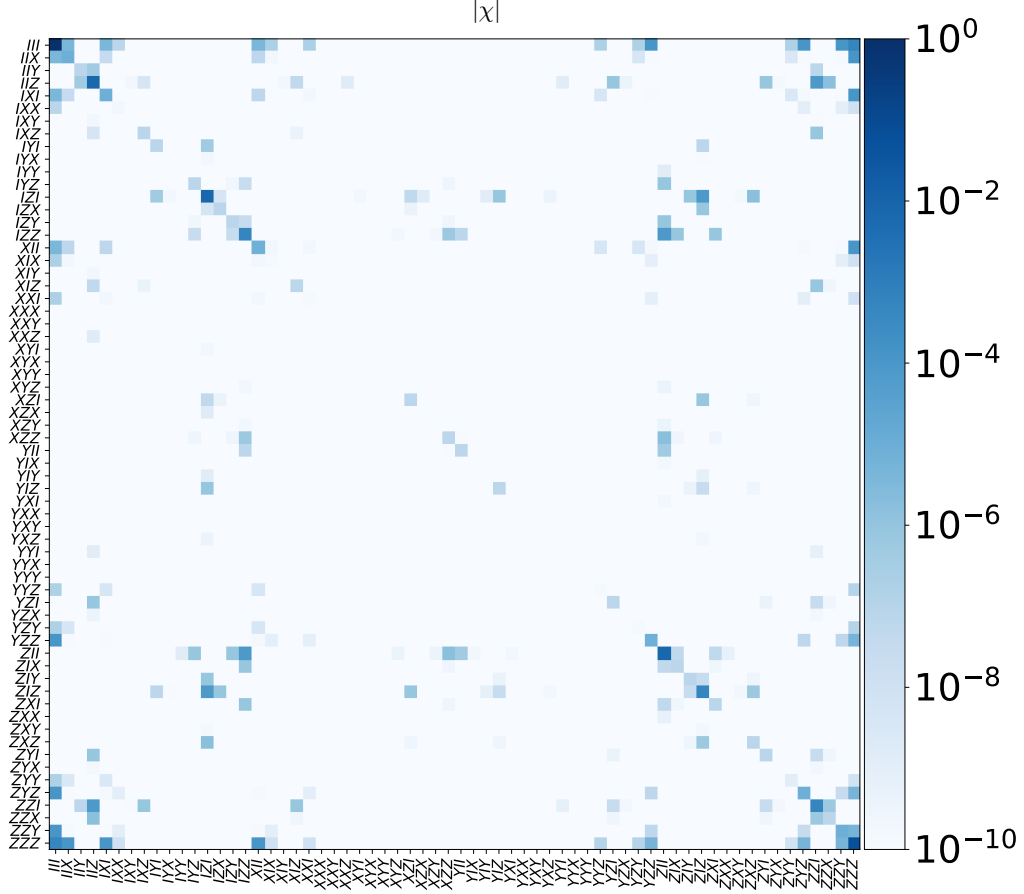


FIG. 13:  $\chi$  error-matrix of the ZZZ gate obtained with simulations based on the second-order reduced model where  $\alpha = 2, \kappa_1 = \frac{\kappa_2}{100}, \epsilon_{ZZZ} = \frac{\kappa_2}{20}$ .

### 3. Hybrid system leakage

For a composite state  $\rho_t = \sum_{d_A} \hat{S}_{A,d_A} \rho_{B,d_A}$  where one subsystem is not actively stabilized, one cannot in general define the leakage on the full system, but only on the stabilized subsystems, or use its full Hilbert space as the code space. But if there is an explicit code space for all the subsystems, then we can apply the definition of the leakage for a composite system introduced in section F2 to this hybrid case. For a bipartite system, we still write the code space as  $I_{c,A} \otimes I_{c,B}$ . At first-order, we have  $\rho_t = \sum_{d_A} \hat{S}_{A,d_A} \rho_{B,d_A} = \sum_{d_A} (\hat{S}_{A,d_A}^{(0)} + \bar{\mathcal{R}}_0(\mathcal{L}_1(\hat{S}_{A,d_A}))) \rho_{B,d_A}$ . And so the leakage  $l$  can be expressed as

$$l = \sum_{d_A} c_{d_A} \text{Tr}(I_{c,B} \rho_{B,d_A})$$

where  $c_{d_A}$  has been defined in Eq. (F2):

$$\begin{aligned} c_{d_A} &= \text{Tr}(\hat{I}_{c,A}(\hat{S}_{A,d_A}^{(0)} + \hat{S}_{A,d_A}^{(1)})) \\ &= \sqrt{2} \delta_{1,d_A} + \text{Tr}(\hat{I}_{c,A} \bar{\mathcal{R}}_0(\mathcal{L}_1(\hat{S}_{A,d_A}))). \end{aligned}$$

### Appendix G: Analytic error models

In this section, we briefly recall the formalism of the Shifted Fock Basis (SFB) introduced in [19] in the context of cat-qubits. We use the decomposition of the cat-qubit into a two-Level System (TLS) and a gauge to derive analytical formulas of phase-flip errors for the ZZZ gate.

The basis is defined as the displacement along the  $+\alpha$  and  $-\alpha$  directions of the Fock states  $|n\rangle$ :

$$|\pm\rangle_L \otimes |n\rangle_g := \mathcal{N}_\pm \left[ \hat{D}(\alpha) \pm (-1)^n \hat{D}(-\alpha) \right] |\hat{n} = n\rangle.$$

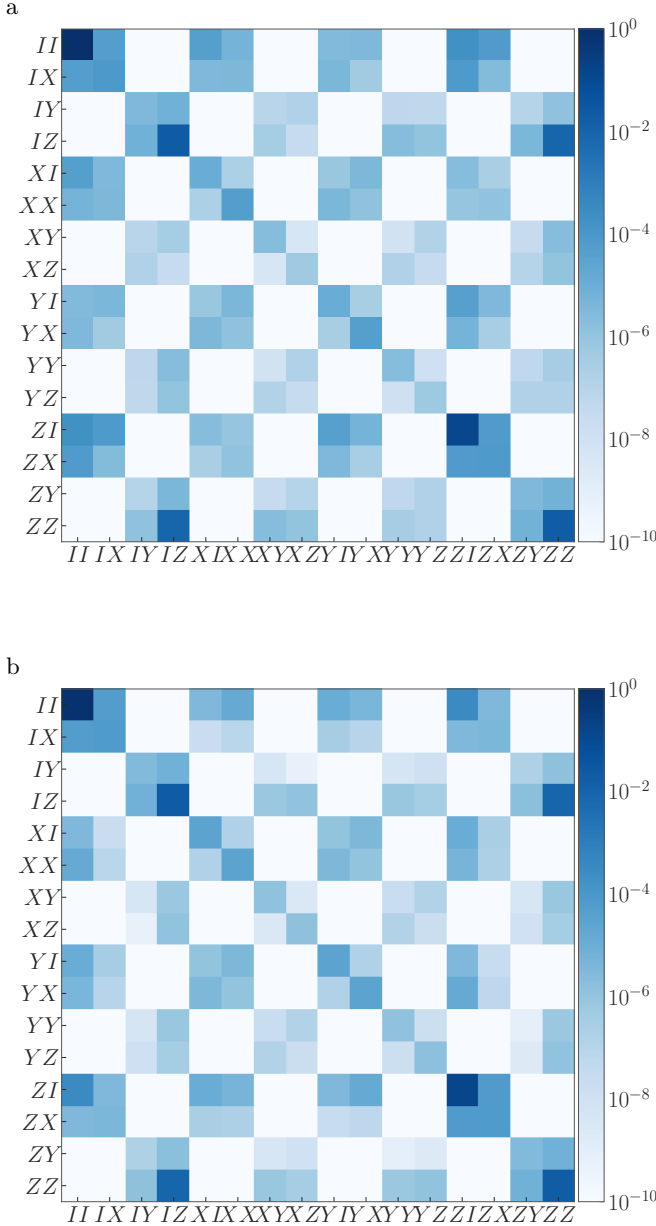


FIG. 14:  $\chi$  error-matrix of the CNOT gate with (a) the full model and (b) the second-order reduced model where  $\alpha = 2$ , and  $\kappa_1 = \kappa_2/100$

We can equivalently think about it as a separation of the full Hilbert space as a direct sum between the even an odd parity spaces or, after relabelling, as a tensor product structure of a logical two level system, a qubit encoding the logical state of the cat mode, and a gauge mode  $\hat{g}$  of another oscillator:

$$\mathcal{H} = \mathbb{C}_L^2 \otimes \mathcal{H}_g.$$

For example, using this basis, the Schrödinger cat states  $|\mathcal{C}_\alpha^\pm\rangle$  are given by:

$$|\mathcal{C}_\alpha^\pm\rangle = |\pm\rangle_L \otimes |0\rangle_g.$$

We will use the following approximation of the annihilation operator, valid for large cat-qubits:

$$\hat{a} \xrightarrow{|\alpha|^2 \gg d} \hat{Z} \otimes (\hat{g}_a + \alpha). \quad (\text{G1})$$

This decomposition of the annihilation operator of the full mode as a  $\hat{Z}$  operator acting on a qubit tensored with a gauge mode  $\hat{g}_a$  is well suited in the perturbative regime where the cat-qubit can be excited to its first excited state, but will quickly decay back to its ground state because of the engineered two-photon dissipation.

Indeed, the operator of the dissipation mechanism  $\hat{a}^2 - |\alpha|^2$  is more intuitive than the annihilation operator because it corresponds to  $2\alpha\hat{I} \otimes \hat{g}$ , i.e. just to cool down the gauge mode  $\hat{g}$  to vacuum.

In the following, we will use these correspondence in order to compute analytical expressions of the  $Z$  errors of the  $Z$  and  $ZZ$  gates used in Sec. II B and Sec. III B, and explicitly derive the analytical expressions of the  $Z$  errors of the  $ZZZ$  gate involving three cat-qubits used in Sec. III C.

### 1. $Z$ and $ZZ$ gates

The analytical expressions of the  $Z$  errors of the  $Z$  gate were derived using the SFB in [19] by adiabatically eliminating the gauge which decays to the ground state manifold with the two-photon dissipation and induces phase flips via the coupling Hamiltonian:  $p_Z = |\alpha|^2 \kappa_1 T + \frac{\epsilon_Z^2 T}{|\alpha|^2 \kappa_2}$ . For a  $ZZ$  gate, the gauges of both modes are adiabatically eliminated independently. The two-photon dissipators with a decay rate  $\kappa = 4|\alpha|^2 \kappa_2$  and the coupling Hamiltonian of rate  $g = \epsilon_{ZZ}$  simplify into a single dissipator with a rate  $2 \cdot 4g^2/\kappa = 2\epsilon_{ZZ}^2/\kappa_2$  causing a  $ZZ$  errors with probability  $p_{Z_a Z_b} = \frac{\pi^2}{8\alpha^4 \kappa_2 T} = \frac{\pi \epsilon_{ZZ}}{2\alpha^2 \kappa_2}$  while the  $Z_a$  and  $Z_b$  errors are pure photon loss errors  $p_{Z_a} = p_{Z_b} = \alpha^2 \kappa_1 T = \frac{\pi \kappa_1}{4\epsilon_{ZZ}}$ . To obtain the total value of  $p_{Z_a Z_b}$ , one has to add the errors due to single photon losses on the two qubits  $p_{Z_a} p_{Z_b}$ .

### 2. $ZZZ$ gate

We first recall the full master equation then write its expression in the SFB before performing an adiabatic elimination of the three gauges to derive the  $ZZZ$  error rate. As detailed in III C, the master equation of this tripartite systems made of three cat-qubits with annihilation operators  $\hat{a}$ ,  $\hat{b}$  and  $\hat{c}$  and gauges  $\hat{g}_a$ ,  $\hat{g}_b$  and  $\hat{g}_c$  is composed of the stabilization  $\mathcal{L}_0$  and perturbations  $\epsilon \mathcal{L}_1$

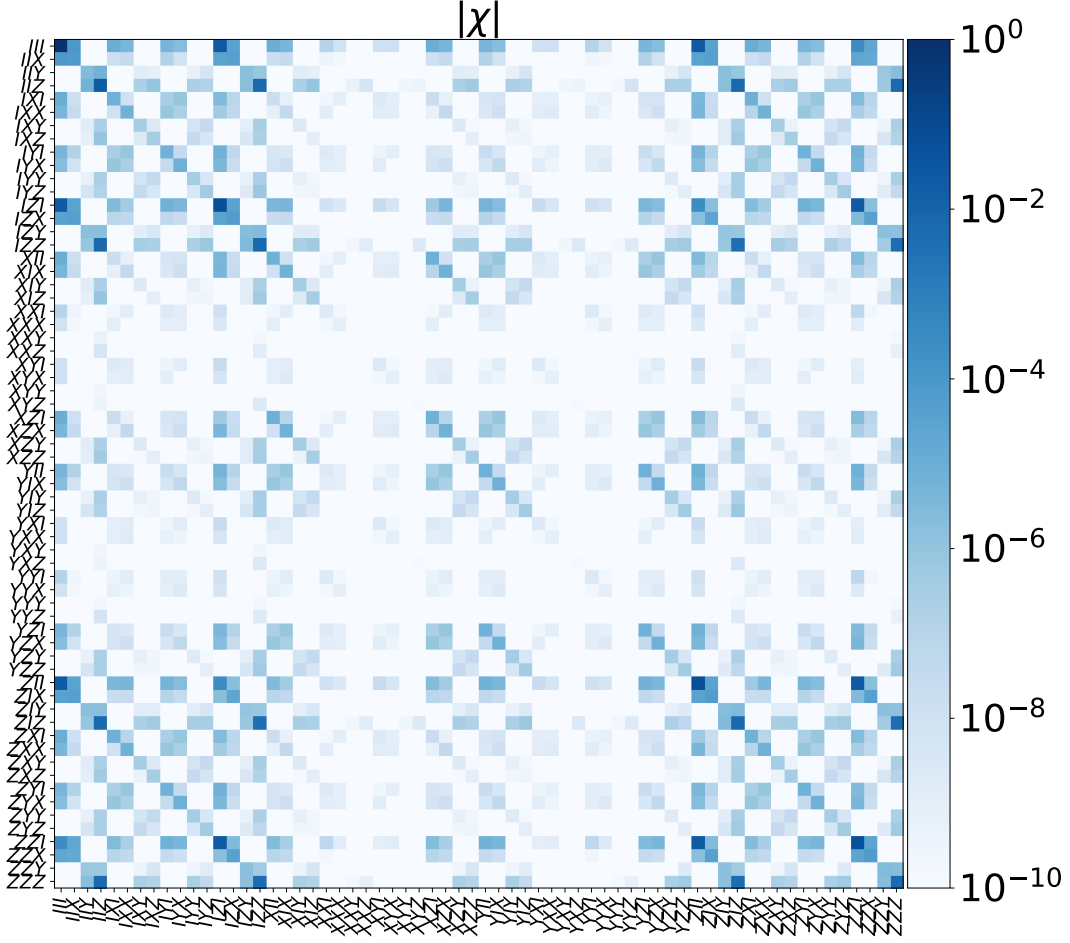


FIG. 15:  $\chi$  error-matrix of the CCNOT gate obtained with simulations based on the second-order reduced model where  $\alpha = 4, \kappa_1 = \frac{\kappa_2}{100}$ . The diagonal elements show the Pauli errors. The top left coefficient displays the fidelity of the gate at 82%. The bottom right coefficient displays the  $ZZZ$  error of the gate at 0.5%.

that can be split between errors and gate dynamics:

$$\begin{aligned}\mathcal{L}_0(\rho) &= \mathcal{D}_{\hat{a}^2 - \alpha^2}(\rho) + \kappa_2 \mathcal{D}_{\hat{b}^2 - \alpha^2}(\rho) + \kappa_2 \mathcal{D}_{\hat{c}^2 - \alpha^2}(\rho), \\ \epsilon \mathcal{L}_1(\rho) &= \kappa_1 \mathcal{D}_{\hat{a}}(\rho) + \kappa_1 \mathcal{D}_{\hat{b}}(\rho) + \kappa_1 \mathcal{D}_{\hat{c}}(\rho) - i [\hat{H}_1, \rho]\end{aligned}$$

where  $\hat{H}_1 = \epsilon_{ZZZ} (\hat{a}\hat{b}\hat{c}^\dagger + \hat{a}^\dagger\hat{b}^\dagger\hat{c})$  is applied for a gate-time  $T = \frac{\pi}{4|\alpha|^3\epsilon_{ZZZ}}$ .

In the SFB, the dissipation writes:

$$\hat{a}^2 - \alpha^2 = \hat{g}_a^2 + 2\alpha\hat{g}_a \sim 2\alpha\hat{g}_a$$

and so the stabilization  $\mathcal{L}_0$  becomes  $4|\alpha|^2\kappa_2(\mathcal{D}_{\hat{g}_a} + \mathcal{D}_{\hat{g}_b} + \mathcal{D}_{\hat{g}_c})(\rho)$ . The one photon loss becomes:  $\kappa_1|\alpha|^2\mathcal{D}_{\hat{Z}_a}(\rho)$ .

The gate dynamics  $\hat{H}_1$  becomes

$$\begin{aligned}2|\alpha|^3\epsilon_{ZZZ}\hat{Z}_a\hat{Z}_b\hat{Z}_c \\ + \epsilon_{ZZZ}|\alpha|^2\hat{Z}_a\hat{Z}_b\hat{Z}_c \otimes (\hat{g}_a + \hat{g}_a^\dagger + \hat{g}_b + \hat{g}_b^\dagger + \hat{g}_c + \hat{g}_c^\dagger).\end{aligned}$$

The first term of the gate dynamics produces the desired rotation. It comes with excitations on the gauges, each with a coupling strength  $g = \epsilon_{ZZZ}|\alpha|^2$ , inflicting a  $ZZZ$  error on the cat-qubits. This excitation decays back to the code space (i.e. ground state of the gauges) with a decay rate  $\kappa = 4|\alpha|^2\kappa_2$  due to  $\mathcal{L}_0$ . In the regime  $\kappa \gg g$ , the gauges remain mainly on their ground states and thus can be adiabatically eliminated, by adding an effective  $ZZZ$  error rate on the qubits with a rate  $3 \times 4g^2/\kappa$ , the factor 3 coming from the three gauges indistinctively. The effective master equation of the effective system  $\rho$

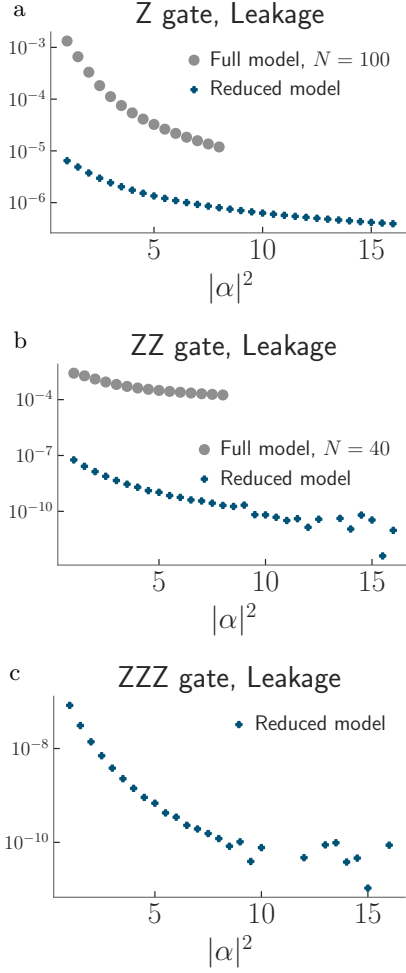


FIG. 16: Leakage of a (a) Z gate, (b) ZZ gate, and (c) ZZZ gate obtained via full model simulations (shown as gray circles) and the reduced model simulations (colored plus) with  $\kappa_1 = \kappa_2/100$ ,  $\epsilon_Z = \kappa_2/20$  for different mean photon number  $|\alpha|^2$ .

therefore becomes:

$$\begin{aligned} \frac{d}{dt}\rho = & \kappa_1|\alpha|^2(\mathcal{D}_{\hat{Z}_a} + \mathcal{D}_{\hat{Z}_b} + \mathcal{D}_{\hat{Z}_c})(\rho(t)) \\ & + \frac{3\epsilon_{ZZZ}|\alpha|^2}{\kappa_2}\mathcal{D}_{\hat{Z}_a\hat{Z}_b\hat{Z}_c}(\rho(t)) \\ & - i\left[2|\alpha|^3\epsilon_{ZZZ}\hat{Z}_a\hat{Z}_b\hat{Z}_c, \rho(t)\right] \end{aligned}$$

The effective Hamiltonian term describes the gate dynamics. We perform a rotation around the ZZZ axis of the qubits with an angle  $\theta = 4|\alpha|^3\epsilon_{ZZZ}T$ . The first terms due to one photon losses induces Z errors on the three cat-qubits:  $p_{Z_a} = p_{Z_b} = p_{Z_c} = |\alpha|^2\kappa_1T$ . The  $Z_aZ_bZ_c$  errors due to the middle term is given by:  $3\frac{\epsilon_{ZZZ}^2|\alpha|^2}{\kappa_2}T = \frac{3\pi\epsilon_{ZZZ}}{4\alpha\kappa_2}$  for a  $\pi$  rotation, to which one has to add the errors due to single photon losses on the three qubits  $p_{Z_a}p_{Z_b}p_{Z_c}$  to obtain the total value of  $p_{Z_aZ_bZ_c}$ .

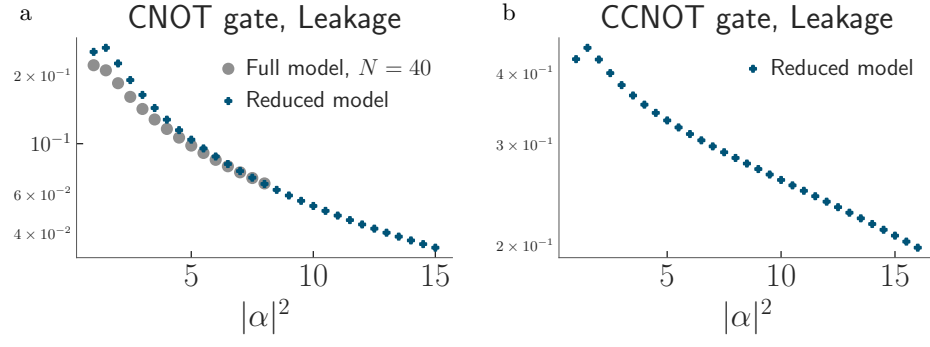


FIG. 17: Leakage of a (a) CNOT gate, and (b) CCNOT gate obtained via full model simulations (shown as gray circles) and the reduced model simulations (colored plus) with  $\kappa_1 = \kappa_2/100$  for different mean photon number  $|\alpha|^2$ .